

NEUTRAL HIGGS BOSON DECAYS TO SQUARK PAIRS REANALYZED

E. Accomando¹, G. Chachamis², F. Fugel², M. Spira² and M. Walser^{2,3}¹ *University of Southampton, Theory Group, Southampton SO17 1BJ, United Kingdom*² *Paul Scherrer Institut, CH-5232 Villigen PSI, Switzerland*³ *Institute for Theoretical Physics, ETH Zürich, CH-8093 Zürich, Switzerland***Abstract**

We analyze neutral Higgs boson decays into squark pairs in the minimal supersymmetric extension of the Standard Model and improve previous analyses. In particular the treatment of potentially large higher-order corrections originating from the soft SUSY breaking parameters A_b , the trilinear Higgs coupling to sbottoms, and μ , the Higgsino mass parameter, is investigated. The remaining theoretical uncertainties including the SUSY-QCD corrections are analyzed quantitatively.

1 Introduction

The search for Higgs bosons plays one of the most important roles at high-energy collider experiments at the Tevatron and the LHC. The Higgs boson is the remnant of electroweak symmetry breaking in the scalar Higgs sector of the Standard Model (SM) and its supersymmetric extensions. The minimal supersymmetric extension of the SM (MSSM) requires the introduction of two Higgs doublets in order to preserve supersymmetry [1]. This leads to the existence of five elementary Higgs particles, two CP-even (h, H), one CP-odd (A) and two charged (H^\pm) states. At lowest order (LO) all couplings and masses of the MSSM Higgs sector are described by two independent input parameters, which are usually chosen as $\tan\beta = v_2/v_1$, the ratio of the two vacuum expectation values $v_{1,2}$, and the pseudoscalar Higgs-boson mass M_A . At LO, the light scalar Higgs mass M_h has to be smaller than the Z -boson mass M_Z . Including the one-loop and dominant two-loop corrections the upper bound is increased to $M_h \lesssim 135$ GeV [2]. Recent first three-loop results confirm this upper bound within less than 1 GeV [3]. The couplings of the various neutral Higgs bosons to fermions and gauge bosons depend on the mixing angles α and β . Normalized to the SM Higgs couplings, they are listed in Table 1. For large values of $\tan\beta$ the down-type Yukawa couplings are strongly enhanced, while the up-type Yukawa couplings are suppressed, unless the light (heavy) scalar Higgs mass ranges at its upper (lower) bound, where the couplings become SM-like.

The negative direct searches for the MSSM Higgs bosons at LEP2 yield lower bounds of $M_{h,H} > 92.8$ GeV and $M_A > 93.4$ GeV. For a SUSY scale $M_{SUSY} = 1$ TeV the range $0.7 < \tan\beta < 2.0$ in the MSSM is excluded by the Higgs searches at the LEP2 experiments [4]. Presently and in the future, Higgs bosons can be searched for at the Fermilab Tevatron [5], a proton-antiproton collider with a center-of-mass energy of 1.96 TeV, and the proton-proton Large Hadron Collider (LHC) with up to 14 TeV center-of-mass energy [6].

Φ		g_u^Φ	g_d^Φ	g_V^Φ
SM	H	1	1	1
MSSM	h	$\cos \alpha / \sin \beta$	$-\sin \alpha / \cos \beta$	$\sin(\beta - \alpha)$
	H	$\sin \alpha / \sin \beta$	$\cos \alpha / \cos \beta$	$\cos(\beta - \alpha)$
	A	$1/\text{tg}\beta$	$\text{tg}\beta$	0

Table 1: *Higgs couplings in the MSSM to fermions and gauge bosons [$V = W, Z$] relative to SM couplings. The subscripts u, d denote up- and down-type fermions.*

The MSSM Higgs bosons couple to squarks, too. If the Higgs masses are large enough to allow for decays into third-generation squark-antisquark pairs, these decay modes acquire sizable branching ratios in many MSSM scenarios [7]. Thus, for a reliable theoretical treatment of these supersymmetric Higgs decay modes, higher order corrections have to be computed and included appropriately. In the past the full SUSY–QCD corrections [8] and the full SUSY–electroweak corrections [9] to the Higgs decays into squarks have been calculated. In particular regions of the MSSM parameter space the corrections turned out to be so large that a reliable prediction was not possible without further refinements. A first attempt to solve this problem has been undertaken in Ref. [10] by starting from a more consistent treatment of the squark masses and couplings at next-to-leading order (NLO). However, the approach of Ref. [10] does not provide a treatment of the squark mixing starting from the running soft SUSY-breaking parameters of the squark sector only. The topic of this work is a complete and consistent determination of the MSSM squark sector and the Higgs couplings to squarks from running \overline{MS} input parameters in the context of SUSY–QCD corrections¹. The input parameters can be obtained from the renormalization group equations in the framework of a certain SUSY-breaking mechanism. Our treatment can also be used for a consistent global fit to supersymmetric observables which include observables based on the stop and sbottom sectors of the MSSM.

This paper is organized as follows. Section 2 describes the systematic determination of the squark sector at NLO, while in Section 3 we summarize the SUSY–QCD corrections to the MSSM Higgs decays into squarks. Numerical results are presented in Section 4. Finally in Section 5 we conclude.

2 Squark masses and couplings

In this section, we describe in detail the determination of the stop and sbottom masses and their couplings to the MSSM Higgs bosons at LO, and extend the setup to NLO consis-

¹We have chosen the \overline{MS} scheme for convenience while our analysis could easily be translated to the \overline{DR} scheme as used in spectrum generators. The \overline{MS} parameters can be obtained from the \overline{DR} ones by simple relations [11] and *vice versa*.

tently. The NLO expressions will be derived for soft supersymmetry breaking parameters given in the \overline{MS} scheme.

2.1 Sfermion masses and couplings at LO

The scalar partners $\tilde{f}_{L,R}$ of the left- and right-handed fermion components mix with each other. The mass eigenstates $\tilde{f}_{1,2}$ of the sfermions \tilde{f} are related to the current eigenstates $\tilde{f}_{L,R}$ by mixing angles θ_f ,

$$\begin{aligned}\tilde{f}_1 &= \tilde{f}_L \cos \theta_f + \tilde{f}_R \sin \theta_f \\ \tilde{f}_2 &= -\tilde{f}_L \sin \theta_f + \tilde{f}_R \cos \theta_f,\end{aligned}\tag{1}$$

which are proportional to the masses of the ordinary fermions, see Eq.(4). Thus mixing effects are only important for the third-generation sfermions $\tilde{t}, \tilde{b}, \tilde{\tau}$, the mass matrix of which is given by

$$\mathcal{M}_{\tilde{f}} = \begin{bmatrix} \tilde{M}_{\tilde{f}_L}^2 + m_f^2 & m_f(A_f - \mu r_f) \\ m_f(A_f - \mu r_f) & \tilde{M}_{\tilde{f}_R}^2 + m_f^2 \end{bmatrix},\tag{2}$$

with the parameters $r_b = r_\tau = 1/r_t = \text{tg}\beta$. The parameter A_f denotes the trilinear sfermion coupling of the soft supersymmetry breaking part of the Lagrangian, while μ is the Higgsino mass parameter and m_f the corresponding fermion mass. The D -terms have been absorbed in the parameters $\tilde{M}_{\tilde{f}_{L/R}}$,

$$\begin{aligned}\tilde{M}_{\tilde{f}_{L/R}}^2 &= M_{\tilde{f}_{L/R}}^2 + D_{\tilde{f}_{L/R}} \\ D_{\tilde{f}_L} &= M_Z^2(I_{3L}^f - e_f \sin^2 \theta_W) \cos 2\beta \\ D_{\tilde{f}_R} &= M_Z^2 e_f \sin^2 \theta_W \cos 2\beta,\end{aligned}\tag{3}$$

where $M_{\tilde{f}_{L/R}}$ denotes the sfermion masses of the soft supersymmetry breaking part of the Lagrangian. Consequently the mixing angles acquire the form

$$\sin 2\theta_f = \frac{2m_f(A_f - \mu r_f)}{m_{\tilde{f}_1}^2 - m_{\tilde{f}_2}^2}, \quad \cos 2\theta_f = \frac{\tilde{M}_{\tilde{f}_L}^2 - \tilde{M}_{\tilde{f}_R}^2}{m_{\tilde{f}_1}^2 - m_{\tilde{f}_2}^2}\tag{4}$$

and the masses of the squark eigenstates are given by

$$m_{\tilde{f}_{1,2}}^2 = m_f^2 + \frac{1}{2} \left[\tilde{M}_{\tilde{f}_L}^2 + \tilde{M}_{\tilde{f}_R}^2 \mp \sqrt{(\tilde{M}_{\tilde{f}_L}^2 - \tilde{M}_{\tilde{f}_R}^2)^2 + 4m_f^2(A_f - \mu r_f)^2} \right].\tag{5}$$

In the current eigenstate basis the neutral Higgs couplings to sfermions read as²

$$\begin{aligned}g_{\tilde{f}_L \tilde{f}_L}^\Phi &= m_f^2 g_1^\Phi + M_Z^2 (I_{3f} - e_f \sin^2 \theta_W) g_2^\Phi \\ g_{\tilde{f}_R \tilde{f}_R}^\Phi &= m_f^2 g_1^\Phi + M_Z^2 e_f \sin^2 \theta_W g_2^\Phi \\ g_{\tilde{f}_L \tilde{f}_R}^\Phi &= -\frac{m_f}{2} (\mu g_3^\Phi - A_f g_4^\Phi)\end{aligned}\tag{6}$$

²In our notation the first index of the neutral Higgs couplings to sfermions defines the incoming and the second index the outgoing sfermion at the corresponding vertex.

with the couplings g_i^Φ ($i = 1, \dots, 4$) listed in Table 2. For the scalar Higgs bosons h, H the couplings to sfermions are symmetric, i.e. $g_{\tilde{f}_R \tilde{f}_L}^{h,H} = g_{\tilde{f}_L \tilde{f}_R}^{h,H}$. For the pseudoscalar Higgs boson A the diagonal couplings $g_{\tilde{f}_L \tilde{f}_L}^A$ and $g_{\tilde{f}_R \tilde{f}_R}^A$ vanish, while the off-diagonal couplings are antisymmetric, i.e. $g_{\tilde{f}_R \tilde{f}_L}^A = -g_{\tilde{f}_L \tilde{f}_R}^A$. The corresponding couplings to the sfermion mass eigenstates $\tilde{f}_{1,2}$ are given by

$$\begin{aligned}
g_{\tilde{f}_1 \tilde{f}_1}^{h,H} &= g_{\tilde{f}_L \tilde{f}_L}^{h,H} \cos^2 \theta_f + g_{\tilde{f}_R \tilde{f}_R}^{h,H} \sin^2 \theta_f + g_{\tilde{f}_L \tilde{f}_R}^{h,H} \sin 2\theta_f \\
g_{\tilde{f}_2 \tilde{f}_2}^{h,H} &= g_{\tilde{f}_L \tilde{f}_L}^{h,H} \sin^2 \theta_f + g_{\tilde{f}_R \tilde{f}_R}^{h,H} \cos^2 \theta_f - g_{\tilde{f}_L \tilde{f}_R}^{h,H} \sin 2\theta_f \\
g_{\tilde{f}_1 \tilde{f}_2}^{h,H} &= g_{\tilde{f}_2 \tilde{f}_1}^{h,H} = \frac{1}{2} (g_{\tilde{f}_R \tilde{f}_R}^{h,H} - g_{\tilde{f}_L \tilde{f}_L}^{h,H}) \sin 2\theta_f + g_{\tilde{f}_L \tilde{f}_R}^{h,H} \cos 2\theta_f \\
g_{\tilde{f}_1 \tilde{f}_1}^A &= g_{\tilde{f}_2 \tilde{f}_2}^A = 0 \\
g_{\tilde{f}_1 \tilde{f}_2}^A &= -g_{\tilde{f}_2 \tilde{f}_1}^A = g_{\tilde{f}_L \tilde{f}_R}^A.
\end{aligned} \tag{7}$$

For a consistent NLO calculation the relations for the sfermion masses, mixing angles and couplings have to be extended to NLO consistently. In the following we will concentrate on the stop and sbottom sectors at NLO SUSY-QCD.

\tilde{f}	Φ	g_1^Φ	g_2^Φ	g_3^Φ	g_4^Φ
\tilde{u}	h	$\cos \alpha / \sin \beta$	$-\sin(\alpha + \beta)$	$-\sin \alpha / \sin \beta$	$\cos \alpha / \sin \beta$
	H	$\sin \alpha / \sin \beta$	$\cos(\alpha + \beta)$	$\cos \alpha / \sin \beta$	$\sin \alpha / \sin \beta$
	A	0	0	1	$-1/\text{tg}\beta$
\tilde{d}	h	$-\sin \alpha / \cos \beta$	$-\sin(\alpha + \beta)$	$\cos \alpha / \cos \beta$	$-\sin \alpha / \cos \beta$
	H	$\cos \alpha / \cos \beta$	$\cos(\alpha + \beta)$	$\sin \alpha / \cos \beta$	$\cos \alpha / \cos \beta$
	A	0	0	1	$-\text{tg}\beta$

Table 2: Coefficients of the neutral MSSM Higgs couplings to sfermion pairs. The symbols \tilde{u}, \tilde{d} denote up- and down-type sfermions.

2.2 Stops and Sbottoms at NLO

The soft supersymmetry-breaking parameters $\overline{M}_{\tilde{q}_{L,R}}(Q_0)$ and $\overline{A}_q(Q_0)$ will be introduced as \overline{MS} parameters at an input scale Q_0 which will in general be of the order of the SUSY scale.

In order to resum large corrections for large values of $\text{tg}\beta$ we define the sbottom masses

and couplings to the Higgs bosons in terms of the effective bottom mass³ [10, 12, 13]

$$\begin{aligned}
\hat{m}_b(Q) &= \frac{\overline{m}_b(Q)}{1 + \Delta_b} \\
\Delta_b &= \frac{C_F}{2} \frac{\alpha_s}{\pi} M_{\tilde{g}} \mu \operatorname{tg}\beta I(m_{\tilde{b}_1}^2, m_{\tilde{b}_2}^2, M_{\tilde{g}}^2) \\
I(a, b, c) &= \frac{ab \log \frac{a}{b} + bc \log \frac{b}{c} + ca \log \frac{c}{a}}{(a-b)(b-c)(a-c)}
\end{aligned} \tag{8}$$

with $C_F = 4/3$, where $\overline{m}_b(Q)$ denotes the running bottom mass in the \overline{MS} scheme at the scale Q and $m_{\tilde{b}_1}, m_{\tilde{b}_2}, M_{\tilde{g}}$ are the sbottom and gluino pole masses respectively. The effective top mass is identified with the running \overline{MS} top mass

$$\hat{m}_t(Q) = \overline{m}_t(Q). \tag{9}$$

The use of these effective masses corresponds to the consistent inclusion of the resummed and RG-improved Yukawa couplings of the Higgs decays $\phi^0 \rightarrow t\bar{t}, b\bar{b}$ everywhere in the squark sectors, too⁴. The stop/sbottom mass matrix at LO is then given by ($q = t, b$)

$$\mathcal{M}_{\tilde{q}} = \begin{bmatrix} \tilde{M}_{\tilde{q}_L}^2(Q_0) + \hat{m}_q^2(Q_0) & \hat{m}_q(Q_0)[\bar{A}_q(Q_0) - \mu r_q] \\ \hat{m}_q(Q_0)[\bar{A}_q(Q_0) - \mu r_q] & \tilde{M}_{\tilde{q}_R}^2(Q_0) + \hat{m}_q^2(Q_0) \end{bmatrix}, \tag{10}$$

where $\bar{A}_q(Q_0)$ denotes the running trilinear \overline{MS} coupling at the scale Q_0 and $r_b = 1/r_t = \operatorname{tg}\beta$. Analogous to Eqs. (3) the D -terms $D_{\tilde{q}_{L/R}}$ have been absorbed in the parameters $\tilde{M}_{\tilde{q}_{L/R}}^2(Q_0)$,

$$\tilde{M}_{\tilde{q}_{L/R}}^2(Q_0) = \overline{M}_{\tilde{q}_{L/R}}^2(Q_0) + D_{\tilde{q}_{L/R}}. \tag{11}$$

The stop/sbottom mass matrix is modified by higher-order corrections in the diagonal and off-diagonal entries. While the corrections to the off-diagonal entries will be treated by the renormalization of the mixing angles, we compensate the radiative corrections to the diagonal matrix elements by shifts in the soft mass parameters $\overline{M}_{\tilde{q}_{L/R}}^2(Q_0)$,

$$M_{\tilde{q}_{L/R}}^2(Q_0) = \overline{M}_{\tilde{q}_{L/R}}^2(Q_0) + \Delta \overline{M}_{\tilde{q}_{L/R}}^2, \quad \tilde{M}_{\tilde{q}_{L/R}}^2(Q_0) = \overline{M}_{\tilde{q}_{L/R}}^2(Q_0) + \Delta \overline{M}_{\tilde{q}_{L/R}}^2 \tag{12}$$

³Note that this definition of the effective bottom quark mass differs from the \overline{DR} definition which has been used in Ref. [10]. Our effective bottom mass runs with five active flavours consistently, i.e. all heavier particles are decoupled, while the \overline{DR} definition requires running with the contributions of all supersymmetric particles. The scale of the strong coupling α_s in Δ_b within the effective bottom mass is identified with the average mass of the sbottom and gluino states in order to account for the NNLO corrections to a large extent [14] and is thus different from the scale Q .

⁴A similar approach has meanwhile been pursued in Ref. [15] for the Higgsino couplings to fermions and sfermions, too.

in order to arrive at simple expressions at NLO for the stop/sbottom masses. Using the squark pole masses $m_{\tilde{q}_{1/2}}$ the tree-level definition $\tilde{\theta}_q$ of the mixing angle is given by

$$\sin 2\tilde{\theta}_q = \frac{2\hat{m}_q(Q_0)[\bar{A}_q(Q_0) - \mu r_q]}{m_{\tilde{q}_1}^2 - m_{\tilde{q}_2}^2} \quad , \quad \cos 2\tilde{\theta}_q = \frac{\tilde{M}_{\tilde{q}_L}^2(Q_0) - \tilde{M}_{\tilde{q}_R}^2(Q_0)}{m_{\tilde{q}_1}^2 - m_{\tilde{q}_2}^2} \quad , \quad (13)$$

where the shifted squark mass parameters $\tilde{M}_{\tilde{q}_{L/R}}(Q_0)$ have been used with the radiatively corrected squark pole masses. This definition will be used as the tree-level-like mixing angle with loop-corrected squark masses $m_{\tilde{q}_{1/2}}$ at NLO, too, but will only play the role of an auxiliary parameter in our analysis as will be explained later.

At NLO the masses of the stop/sbottom eigenstates are given by

$$\begin{aligned} m_{\tilde{q}_{1/2}}^2 &= \hat{m}_q^2(Q_0) + \frac{1}{2} \left[\tilde{M}_{\tilde{q}_L}^2(Q_0) + \tilde{M}_{\tilde{q}_R}^2(Q_0) \right. \\ &\quad \left. \mp \sqrt{[\tilde{M}_{\tilde{q}_L}^2(Q_0) - \tilde{M}_{\tilde{q}_R}^2(Q_0)]^2 + 4\hat{m}_q^2(Q_0)[\bar{A}_q(Q_0) - \mu r_q]^2} \right] + \Delta m_{\tilde{q}_{1/2}}^2 \\ \Delta m_{\tilde{q}_{1/2}}^2 &= \Sigma_{11/22}(m_{\tilde{q}_{1/2}}^2) + \delta\hat{m}_{\tilde{q}_{1/2}}^2 \end{aligned} \quad (14)$$

The diagonal parts $\Sigma_{11/22}$ of the stop/sbottom self-energies can be calculated from the diagrams in Fig. 1,

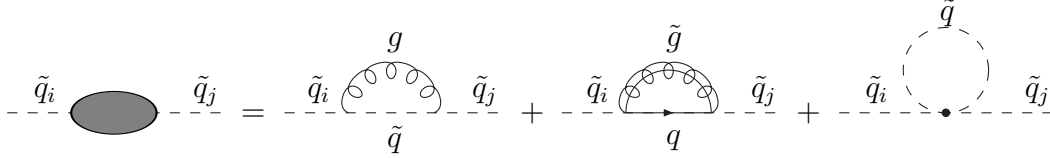


Figure 1: *One-loop contributions to the squark self-energies.*

$$\begin{aligned} \Sigma_{11/22}(m_{\tilde{q}_{1/2}}^2) &= C_F \frac{\alpha_s}{\pi} \frac{1}{4} \left\{ -(1 + \cos^2 2\tilde{\theta}_q) A_0(m_{\tilde{q}_{1/2}}) - \sin^2 2\tilde{\theta}_q A_0(m_{\tilde{q}_{2/1}}) \right. \\ &\quad \left. + 2A_0(M_{\tilde{g}}) + 2A_0[\hat{m}_q(Q_0)] + 4m_{\tilde{q}_{1/2}}^2 B_0(m_{\tilde{q}_{1/2}}^2; 0, m_{\tilde{q}_{1/2}}) \right. \\ &\quad \left. + 2 \left[M_{\tilde{g}}^2 + \hat{m}_q^2(Q_0) - m_{\tilde{q}_{1/2}}^2 \mp 2M_{\tilde{g}}\hat{m}_q(Q_0) \sin 2\tilde{\theta}_q \right] B_0[m_{\tilde{q}_{1/2}}^2; M_{\tilde{g}}, \hat{m}_q(Q_0)] \right\} . \end{aligned} \quad (15)$$

The one-loop integrals are defined as [16]

$$\begin{aligned} A_0(m) &= \int \frac{d^n k}{(2\pi)^n} \frac{-i(4\pi)^2 \bar{\mu}^{2\epsilon}}{k^2 - m^2} \\ B_0(p^2; m_1, m_2) &= \int \frac{d^n k}{(2\pi)^n} \frac{-i(4\pi)^2 \bar{\mu}^{2\epsilon}}{[k^2 - m_1^2][(k+p)^2 - m_2^2]} \\ B_1(p^2; m_1, m_2) &= \frac{1}{2p^2} \left\{ A_0(m_1) - A_0(m_2) - (p^2 + m_1^2 - m_2^2) B_0(p^2; m_1, m_2) \right\} . \end{aligned} \quad (16)$$

The parameter $\bar{\mu}$ denotes the 't Hooft mass of dimensional regularization. The counter terms $\delta\hat{m}_{\tilde{q}_{1,2}}^2$ are given by

$$\begin{aligned}
\delta\hat{m}_{\tilde{q}_{1/2}}^2 &= 2\hat{m}_q(Q_0)\delta\hat{m}_q + \frac{1}{2} \left\{ \delta\bar{M}_{\tilde{q}_L}^2 + \delta\bar{M}_{\tilde{q}_R}^2 \pm \left[(\delta\bar{M}_{\tilde{q}_L}^2 - \delta\bar{M}_{\tilde{q}_R}^2) \cos 2\tilde{\theta}_q \right. \right. \\
&\quad \left. \left. + \left(\frac{\delta\hat{m}_q}{\hat{m}_q(Q_0)} + \frac{\delta\bar{A}_q}{\bar{A}_q(Q_0) - \mu r_q} \right) (m_{\tilde{q}_1}^2 - m_{\tilde{q}_2}^2) \sin^2 2\tilde{\theta}_q \right] \right\} \\
&= -C_F \frac{\alpha_s}{\pi} \Gamma(1 + \epsilon) (4\pi)^\epsilon \left\{ \frac{1}{\epsilon} + \log \frac{\bar{\mu}^2}{Q_0^2} \right\} \left\{ M_{\tilde{g}}^2 \mp M_{\tilde{g}} \hat{m}_q(Q_0) \sin 2\tilde{\theta}_q \right\} \\
&\quad + \frac{\delta\hat{m}_q}{\hat{m}_q(Q_0)} \left\{ 2\hat{m}_q^2(Q_0) \mp \frac{1}{2} (m_{\tilde{q}_2}^2 - m_{\tilde{q}_1}^2) \sin^2 2\tilde{\theta}_q \right\}, \tag{17}
\end{aligned}$$

where the tree-level-like mixing angle $\tilde{\theta}_q$ of Eq. (13) has been used and the parameters $\bar{M}_{\tilde{q}_{L/R}}^2$ and \bar{A}_q have been renormalized in the \overline{MS} scheme,

$$\begin{aligned}
\delta\bar{M}_{\tilde{q}_{L/R}}^2 &= -C_F \frac{\alpha_s}{\pi} \Gamma(1 + \epsilon) (4\pi)^\epsilon M_{\tilde{g}}^2 \left\{ \frac{1}{\epsilon} + \log \frac{\bar{\mu}^2}{Q_0^2} \right\} \\
\delta\bar{A}_q &= C_F \frac{\alpha_s}{\pi} \Gamma(1 + \epsilon) (4\pi)^\epsilon M_{\tilde{g}} \left\{ \frac{1}{\epsilon} + \log \frac{\bar{\mu}^2}{Q_0^2} \right\}. \tag{18}
\end{aligned}$$

The counter term of the effective quark mass $\hat{m}_q(Q)$ for $Q = Q_0$ is given by⁵

$$\begin{aligned}
\frac{\delta\hat{m}_q}{\hat{m}_q(Q)} &= -C_F \frac{\alpha_s}{\pi} \Gamma(1 + \epsilon) (4\pi)^\epsilon \frac{3}{4} \left\{ \frac{1}{\epsilon} + \log \frac{\bar{\mu}^2}{Q^2} + \delta_{SUSY} \right\} + \Delta_q \\
&\quad - C_F \frac{\alpha_s}{4\pi} \left\{ B_1[\hat{m}_q^2(Q); M_{\tilde{g}}, m_{\tilde{q}_1}] + B_1[\hat{m}_q^2(Q); M_{\tilde{g}}, m_{\tilde{q}_2}] \right. \\
&\quad \left. + 2M_{\tilde{g}}(\bar{A}_q - \mu r_q) \frac{B_0[\hat{m}_q^2(Q); M_{\tilde{g}}, m_{\tilde{q}_1}] - B_0[\hat{m}_q^2(Q); M_{\tilde{g}}, m_{\tilde{q}_2}]}{m_{\tilde{q}_1}^2 - m_{\tilde{q}_2}^2} \right\}, \tag{19}
\end{aligned}$$

where $\delta_{SUSY} = 1/3$ is a finite counter term required to restore the supersymmetric relations between the Higgs boson couplings to top/bottom quarks and stops/sbottoms within dimensional regularization [11]. The term Δ_q denotes the correction Δ_b of Eq. (8) for the bottom mass, while it vanishes for the top mass case, i.e. $\Delta_t = 0$. The term Δ_b in the counter term of the bottom mass cancels the leading term for large values of $\text{tg}\beta$ in the last line of Eq. (19) so that this counter term is free of large corrections. Using the NLO corrected squark pole masses of Eq. (14) and the tree-level-like mixing angle $\tilde{\theta}_q$ of Eq. (13), the shifted squared soft SUSY-breaking squark mass parameters

⁵The quark mass counter term is different from the \overline{DR} expression used in Ref. [10].

$\tilde{M}_{\tilde{q}_{L/R}}^2(Q_0) = \tilde{\bar{M}}_{\tilde{q}_{L/R}}^2(Q_0) + \Delta\bar{M}_{\tilde{q}_{L/R}}^2$ can be obtained from the relations⁶,

$$\begin{aligned}\tilde{M}_{\tilde{q}_L}^2(Q_0) &= M_{\tilde{q}_L}^2(Q_0) + D_{\tilde{q}_L} = m_{\tilde{q}_1}^2 \cos^2 \tilde{\theta}_q + m_{\tilde{q}_2}^2 \sin^2 \tilde{\theta}_q - \hat{m}_q^2(Q_0) \\ \tilde{M}_{\tilde{q}_R}^2(Q_0) &= M_{\tilde{q}_R}^2(Q_0) + D_{\tilde{q}_R} = m_{\tilde{q}_1}^2 \sin^2 \tilde{\theta}_q + m_{\tilde{q}_2}^2 \cos^2 \tilde{\theta}_q - \hat{m}_q^2(Q_0).\end{aligned}\quad (20)$$

The tree-level definition of the mixing angle $\tilde{\theta}_q$ in Eq. (13) corresponds to the following counter term at NLO,

$$\delta\tilde{\theta}_q = \frac{\text{tg } 2\tilde{\theta}_q}{2} \left\{ \frac{\delta\hat{m}_q}{\hat{m}_q(Q_0)} + \frac{\delta\bar{A}_q}{\bar{A}_q(Q_0) - \mu r_q} - \frac{\delta m_{\tilde{q}_1}^2 - \delta m_{\tilde{q}_2}^2}{m_{\tilde{q}_1}^2 - m_{\tilde{q}_2}^2} \right\}, \quad (21)$$

$$\delta m_{\tilde{q}_{1/2}}^2 = -\Sigma_{11/22}(m_{\tilde{q}_{1/2}}^2). \quad (22)$$

However, in order to avoid artificial singularities in physical observables for stop/sbottom masses $m_{\tilde{q}_{1,2}}$ close to each other, in our calculation the mixing angle of the squark fields has been renormalized via the anti-Hermitian counter term⁷ [8, 10],

$$\delta\theta_q = \frac{1}{2} \frac{\Re\Sigma_{12}(m_{\tilde{q}_1}^2) + \Re\Sigma_{12}(m_{\tilde{q}_2}^2)}{m_{\tilde{q}_2}^2 - m_{\tilde{q}_1}^2}, \quad (23)$$

where Σ_{12} denotes the off-diagonal part of the stop/sbottom self-energy (see Fig. 1) describing transitions from the first to the second mass eigenstate or *vice versa*,

$$\begin{aligned}\Sigma_{12}(m^2) &= -C_F \frac{\alpha_s}{\pi} \left\{ M_{\tilde{g}} \hat{m}_q(Q_0) B_0[m^2; M_{\tilde{g}}, \hat{m}_q(Q_0)] \right. \\ &\quad \left. + \frac{\sin 2\tilde{\theta}_q}{4} [A_0(m_{\tilde{q}_2}) - A_0(m_{\tilde{q}_1})] \right\} \cos 2\tilde{\theta}_q.\end{aligned}\quad (24)$$

This implies a finite shift $\Delta\tilde{\theta}_q$ to the mixing angle $\tilde{\theta}_q$ of Eq. (13),

$$\theta_q = \tilde{\theta}_q + \Delta\tilde{\theta}_q, \quad \Delta\tilde{\theta}_q = \delta\tilde{\theta}_q - \delta\theta_q \quad (25)$$

which modifies the relations of Eq. (20) by replacing $\tilde{\theta}_q = \theta_q - \Delta\tilde{\theta}_q$. The scale and scheme dependence of the input parameters determining the squark pole masses is explicitly

⁶These equations differ from the corresponding inconsistent relations in terms of the on-shell definition of the mixing angle used in [10]. Our approach starts from the consistent tree-level relations and incorporates the anti-Hermitian definition of the mixing angle in a finite shift from the tree-level value $\tilde{\theta}_q$. An alternative and equivalent option would be to compensate the shift $\Delta\tilde{\theta}_q$ by a shifted trilinear coupling A_q . Moreover, it should be noted that the shifted parameters $M_{\tilde{t}_L}(Q_0)$ and $M_{\tilde{b}_L}(Q_0)$ are not equal to each other any more in accordance with the different radiative corrections to the stop and sbottom masses.

⁷Alternatively the mixing angle can be renormalized by the counter term $\delta\theta_q = \Re\Sigma_{12}(Q^2)/(m_{\tilde{q}_2}^2 - m_{\tilde{q}_1}^2)$ with $Q^2 = m_{\tilde{q}_1}^2$ or $Q^2 = m_{\tilde{q}_2}^2$ [17] which leads to a result free of the artificial singularities for stop/sbottom masses $m_{\tilde{q}_{1,2}}$ close to each other, too. Another option free of these singularities is provided by taking the residue of Eq. (23) for equal masses for the mixing angle counter term [18].

compensated by the corrections $\Delta m_{\tilde{q}_{1,2}}^2$ to the tree-level relations of Eq. (14), while the scale dependence of the mixing angle is compensated by the finite shift $\Delta\tilde{\theta}_q$ in Eq. (25). It should be noted that the corrected mixing angle fulfills the relation $\sin^2 2\theta_q + \cos^2 2\theta_q = 1$ at NLO consistently which will be necessary for the cancellation of the ultraviolet divergences of the NLO corrections to Higgs decays into squarks. The scale of the strong coupling constants α_s in Eqs. (15, 17, 18, 19, 24) has been identified with the input scale Q_0 .

In order to obtain fully consistent input parameters Eqs. (8, 13, 14, 20) would have to be solved iteratively until the squark pole masses do not change anymore. Performing this iteration explicitly, however, shows that for certain MSSM scenarios convergence cannot be reached. This happens in particular for scenarios where the parameters $M_{\tilde{q}_L}^2$ and $M_{\tilde{q}_R}^2$ are close to each other so that the mixing angle $\tilde{\theta}_q$ is driven towards $\pm\pi/4$ and $\Delta m_{\tilde{q}_2}^2$ towards $-\Delta m_{\tilde{q}_1}^2$. This leads to a situation in which the squark pole masses do not change anymore, but the mixing angles $\tilde{\theta}_q, \theta_q$ do not correspond to the relations of Eqs. (13, 25) so that the iterated parameters are inconsistent. This situation can be avoided by stopping the iteration earlier before running into this inconsistent limit. Since the iteration adds contributions beyond NLO to the input parameters and the squark masses, the iteration effects can be considered as arbitrary in a NLO analysis. We have chosen a procedure where no iteration is performed as described above. With the shifted parameters $\tilde{M}_{\tilde{q}_{L,R}}^2$ of Eq. (20) the squark pole masses are calculated by Eq. (14) with vanishing $\Delta m_{\tilde{q}_{1,2}}^2$ terms and the mixing angles according to Eqs. (13, 25), since the NLO corrections are absorbed in the shifted values for $\tilde{M}_{\tilde{q}_{L,R}}^2$. However, for a consistent treatment of the Δ_q terms of Eq. (8) iterations for the effective bottom mass $\hat{m}_b(Q_0)$ are performed for the sbottom sector. This ensures that the effective bottom mass of the corrected mass matrix corresponds to the NLO sbottom pole masses consistently.

The NLO neutral Higgs couplings to squarks read in the current eigenstate basis as

$$\begin{aligned}
g_{\tilde{q}_L\tilde{q}_L}^\Phi(\mu_R) &= \hat{m}_q^2(\mu_R)g_1^\Phi + M_Z^2(I_{3q} - e_q \sin^2 \theta_W)g_2^\Phi \\
g_{\tilde{q}_R\tilde{q}_R}^\Phi(\mu_R) &= \hat{m}_q^2(\mu_R)g_1^\Phi + M_Z^2 e_q \sin^2 \theta_W g_2^\Phi \\
g_{\tilde{q}_L\tilde{q}_R}^\Phi(\mu_R) &= -\frac{\hat{m}_q(\mu_R)}{2} [\mu g_3^\Phi - \bar{A}_q(\mu_R)g_4^\Phi]
\end{aligned} \tag{26}$$

with the couplings g_i^Φ listed in Table 2. Note that we use a common renormalization scale μ_R for the effective quark mass \hat{m}_q and the trilinear coupling \bar{A}_q for simplicity. The corresponding couplings to the stop/sbottom mass eigenstates $\tilde{q}_{1,2}$ are obtained by the appropriate rotations according to Eq. (7) by the on-shell mixing angle θ_q of Eq. (25). The choice of the on-shell mixing angle θ_q for these rotations implies that this is also the relevant mixing angle involved in the physical processes. The on-shell mixing angle is uniquely related to the soft SUSY-breaking input parameters according to Eqs. (13,25) and thus in particular to the parameter A_q .

In our numerical analysis we include the running of the effective quark mass \hat{m}_q and the trilinear coupling \bar{A}_q up to the NLL level in (SUSY-)QCD. Note that due to the counter terms for the effective quark masses of Eq. (19) the heavy particles are decoupled from

its running. We have included 5 (6) light flavours in the NLL running of the effective bottom (top) masses. For the running of the trilinear couplings \bar{A}_q we have kept the contributions of all coloured particles including the top quark, the squarks and the gluino which is consistent with the counter term $\delta\bar{A}_q$ of Eq. (18). The running effective quark mass for $N_F = 5, 6$ light flavours is thus given by

$$\begin{aligned}\hat{m}_q(\mu_R) &= \hat{m}_q(m_q) \frac{c[\alpha_s(\mu_R)/\pi]}{c[\alpha_s(m_q)/\pi]} \\ c(x) &= \left(\frac{23}{6}x\right)^{\frac{12}{23}} \left[1 + \frac{3731}{3174}x\right] \quad \text{for } q = b \quad (N_F = 5) \\ c(x) &= \left(\frac{7}{2}x\right)^{\frac{4}{7}} \left[1 + \frac{137}{98}x\right] \quad \text{for } q = t \quad (N_F = 6),\end{aligned}\quad (27)$$

where m_q denotes the corresponding quark pole mass. The NLL evolution of the trilinear couplings \bar{A}_q with $N_F = 6$ quark and squark flavours is determined as the solution of the corresponding two-loop renormalization group equations (RGEs) with respect to the strong coupling constant [11, 19] and can be expressed as⁸

$$\begin{aligned}\bar{A}_q(\mu_R) &= \bar{A}_q(Q_0) + M_3(Q_0) \left\{ -\frac{16}{9} \left[\frac{\alpha_{s,SUSY}(\mu_R)}{\alpha_{s,SUSY}(Q_0)} - 1 \right] \left[1 + \frac{1}{6} \frac{\alpha_{s,SUSY}(Q_0)}{\pi} \right] \right. \\ &\quad \left. - \frac{16}{27} \frac{\alpha_{s,SUSY}(Q_0)}{\pi} \left[\frac{\alpha_{s,SUSY}^2(\mu_R)}{\alpha_{s,SUSY}^2(Q_0)} - 1 \right] \right\}\end{aligned}\quad (28)$$

with the running strong coupling $\alpha_{s,SUSY}$ including all quarks, squarks and gluinos,

$$\alpha_{s,SUSY}(\mu) = \frac{12\pi}{9 \log(\mu^2/\Lambda_{SUSY}^2)} \left\{ 1 - \frac{14}{9} \frac{\log \log(\mu^2/\Lambda_{SUSY}^2)}{\log(\mu^2/\Lambda_{SUSY}^2)} \right\}, \quad (29)$$

where Λ_{SUSY} is determined by the matching condition

$$\alpha_{s,SUSY}(Q_0) = \alpha_s(Q_0) \left\{ 1 + \frac{\alpha_s(Q_0)}{\pi} \left[\frac{1}{6} \log \frac{Q_0^2}{m_t^2} + \frac{1}{2} \log \frac{Q_0^2}{M_{\tilde{g}}^2} + \frac{1}{24} \sum_{\tilde{q}_i} \log \frac{Q_0^2}{m_{\tilde{q}_i}^2} \right] \right\} \quad (30)$$

between the strong coupling $\alpha_{s,SUSY}$ including all quarks, squarks and gluinos and the low-energy QCD couplings α_s with 5 active light flavours. The \overline{MS} mass $M_3(Q_0)$ of the gluino can be obtained from the gluino pole mass $M_{\tilde{g}}$,

$$\begin{aligned}M_3(Q_0) &= M_{\tilde{g}} \left\{ 1 - \frac{\alpha_s(M_{\tilde{g}})}{\pi} \left[C_A + \frac{3}{4} C_A \log \frac{Q_0^2}{M_{\tilde{g}}^2} \right. \right. \\ &\quad \left. \left. + \frac{1}{4} \sum_{q,i} \left(B_1(M_{\tilde{g}}^2; m_q, m_{\tilde{q}_i}) + \frac{\Gamma(1+\epsilon)(4\pi)^\epsilon}{2\epsilon} + \frac{1}{2} \log \frac{\bar{\mu}^2}{Q_0^2} \right. \right. \right. \\ &\quad \left. \left. \left. - (-1)^i \frac{m_q}{M_{\tilde{g}}} \sin 2\theta_q B_0(M_{\tilde{g}}^2; m_q, m_{\tilde{q}_i}) \right) \right] \right\},\end{aligned}\quad (31)$$

⁸Note that the RGEs have been transformed into the \overline{MS} scheme appropriately [11]. In the \overline{DR} scheme the coefficient 1/6 is replaced by 7/6, the coefficient 16/27 by 4/27 and the \overline{MS} gluino mass $M_3(Q_0)$ by the corresponding \overline{DR} gluino mass in Eq. (28).

where $C_A = 3$. The sum is performed over all 3 (s)quark generations. For the first two generations we neglected the quark masses in the squark mass matrices so that the corresponding squark pole masses are given by

$$m_{\tilde{q}_{L/R}}^2 = \tilde{M}_{\tilde{q}_{L/R}}^2(Q_0) + C_F \frac{\alpha_s(Q_0)}{\pi} \left\{ M_{\tilde{g}}^2 \log \frac{Q_0^2}{M_{\tilde{g}}^2} + \frac{\tilde{M}_{\tilde{q}_{L/R}}^2(Q_0)}{2} \log \frac{M_{\tilde{g}}^2}{\tilde{M}_{\tilde{q}_{L/R}}^2(Q_0)} \right. \\ \left. + \frac{1}{2} \tilde{M}_{\tilde{q}_{L/R}}^2(Q_0) + \frac{3}{2} M_{\tilde{g}}^2 + \frac{\left[M_{\tilde{g}}^2 - \tilde{M}_{\tilde{q}_{L/R}}^2(Q_0) \right]^2}{2 \tilde{M}_{\tilde{q}_{L/R}}^2(Q_0)} \log \left| \frac{M_{\tilde{g}}^2 - \tilde{M}_{\tilde{q}_{L/R}}^2(Q_0)}{M_{\tilde{g}}^2} \right| \right\} \quad (32)$$

3 Results at NLO

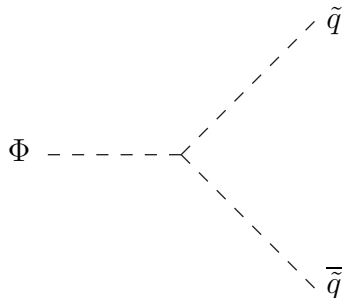


Figure 2: *MSSM Higgs boson decays into squark-antisquark pairs at leading order.*

At leading order the MSSM Higgs boson decays into squark-antisquark pairs are described by the diagram shown in Fig. 2. The corresponding partial decay width reads as

$$\Gamma_{LO}(\Phi \rightarrow \tilde{q}_i \bar{\tilde{q}}_j) = \frac{N_c G_F}{2\sqrt{2}\pi M_\Phi} \left[g_{\tilde{q}_i \bar{\tilde{q}}_j}^\Phi(\mu_R) \right]^2 \sqrt{\lambda_{ij}} \quad (33)$$

with the two-body phase-space function

$$\lambda_{ij} = \left(1 - \frac{m_{\tilde{q}_i}^2}{M_\Phi^2} - \frac{m_{\tilde{q}_j}^2}{M_\Phi^2} \right)^2 - 4 \frac{m_{\tilde{q}_i}^2 m_{\tilde{q}_j}^2}{M_\Phi^4}. \quad (34)$$

While Higgs boson decays into squarks of the first two generations are generally suppressed, Higgs decays into sbottoms and stops develop sizable branching ratios, whenever they are kinematically possible [7]. In particular scenarios their branching ratios can reach a level of 80–90% [7, 8, 20].

The SUSY–QCD corrections at NLO have been calculated in Refs. [8]. However, the analytical results will be repeated in this section in our notation and for the investigation of calculational details once consistent input parameters at NLO are included in the theoretical analysis. The SUSY–QCD corrections consist of one-loop virtual corrections,

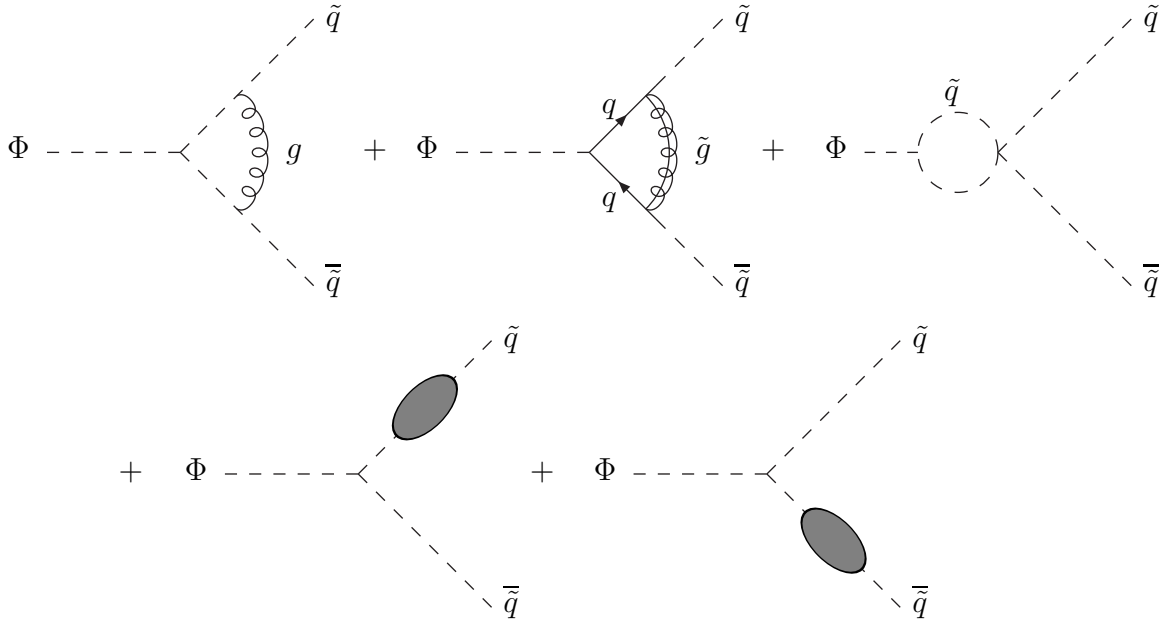


Figure 3: *Virtual corrections to MSSM Higgs boson decays into squark-antisquark pairs at next-to-leading order. The external self-energy blobs represent the self-energy diagrams of Fig. 1.*

mediated by the Feynman diagrams depicted in Fig. 3, supplemented by the renormalization of the mass, coupling and wave function parameters involved, and real corrections due to gluon bremsstrahlung, see Fig. 4. We have performed the loop and phase-space integration within dimensional regularization in $n = 4 - 2\epsilon$ dimensions so that ultraviolet and infrared singularities appear as poles in ϵ . The infrared singularities cancel after adding the real and virtual corrections. The ultraviolet poles disappear after adding the corresponding counter terms which will be discussed in detail in the following, since they have to correspond to the schemes in which the squark masses, mixing angles and couplings are defined.

The wave-function counter terms δZ_{ii} ($i = 1, 2$) are determined by normalizing the residues of the diagonalized squark propagators to unity. The explicit calculation of the diagrams of Fig. 1 leads to the expressions

$$\delta Z_{ii} = \frac{C_F \alpha_s}{2\pi} \left\{ B_0(m_{\tilde{q}_i}^2; 0, m_{\tilde{q}_i}) - B_0(m_{\tilde{q}_i}^2; M_{\tilde{g}}, m_q) + 2m_{\tilde{q}_i}^2 B'_0(m_{\tilde{q}_i}^2; 0, m_{\tilde{q}_i}) \right. \\ \left. + [M_{\tilde{g}}^2 + m_q^2 - m_{\tilde{q}_i}^2 + (-1)^i 2M_{\tilde{g}} m_q \sin 2\theta_q] B'_0(m_{\tilde{q}_i}^2; M_{\tilde{g}}, m_q) \right\}, \quad (35)$$

where the derivative of the two-point function is defined as

$$B'_0(p^2; m_1, m_2) = \frac{\partial}{\partial p^2} B_0(p^2; m_1, m_2). \quad (36)$$

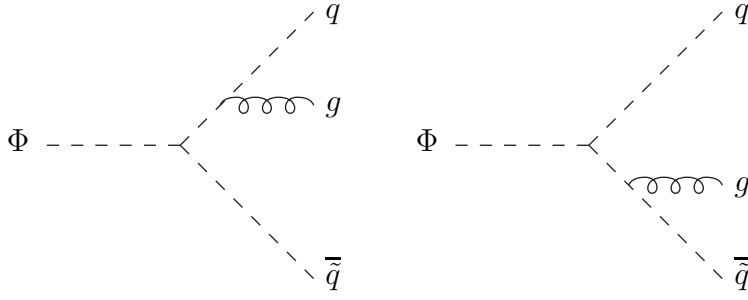


Figure 4: *Real corrections to MSSM Higgs boson decays into squark-antisquark pairs at next-to-leading order.*

Throughout our calculation in this section the quark mass m_q is defined as $\hat{m}_b(\mu_R)$ of Eq. (8) for decays into sbottom pairs and as $\hat{m}_t(\mu_R)$ of Eq. (9) for decays into stops. The mixing angle is renormalized by the anti-Hermitian counter term of Eq. (23). The trilinear couplings $\bar{A}_q(\mu_R)$ ($q = b, t$) are defined in the \overline{MS} scheme at the scale μ_R which is identical to the running couplings in the \overline{DR} definition at NLO. Thus, the counter term of $\bar{A}_q(\mu_R)$ can be cast into the form

$$\delta\bar{A}_q = C_F \frac{\alpha_s}{\pi} \Gamma(1 + \epsilon) (4\pi)^\epsilon M_{\tilde{g}} \left\{ \frac{1}{\epsilon} + \log \frac{\bar{\mu}^2}{\mu_R^2} \right\}. \quad (37)$$

The quark mass counter term δm_q is given by

$$\delta m_q = \delta \hat{m}_q \quad (38)$$

with the top and bottom mass counter terms $\delta \hat{m}_q$ of Eq. (19) with $Q = \mu_R$.

The calculation of the diagrams of Fig. 3 for the virtual corrections and those of Fig. 4 for the real corrections leads to the final result after renormalization,

$$\begin{aligned} \Gamma(\Phi \rightarrow \tilde{q}_i \bar{\tilde{q}}_j) &= \Gamma_{LO}(\Phi \rightarrow \tilde{q}_i \bar{\tilde{q}}_j) \left\{ 1 + C^\Phi \frac{\alpha_s}{\pi} \right\} \\ C^\Phi &= \frac{C_F}{2} [C_1^\Phi + C_2^\Phi + C_3^\Phi] + C_{CT}^\Phi + C_{real}^\Phi \\ C_1^\Phi &= B_0(m_{\tilde{q}_i}^2; 0, m_{\tilde{q}_i}) + B_0(m_{\tilde{q}_j}^2; 0, m_{\tilde{q}_j}) - B_0(M_\Phi^2; m_{\tilde{q}_i}, m_{\tilde{q}_j}) \\ &\quad - 2(M_\Phi^2 - m_{\tilde{q}_i}^2 - m_{\tilde{q}_j}^2) C_0(m_{\tilde{q}_i}^2, M_\Phi^2, m_{\tilde{q}_j}^2; 0, m_{\tilde{q}_i}, m_{\tilde{q}_j}) \\ C_2^{h,H} &= \frac{g_q^{h,H}}{g_{\tilde{q}_i \tilde{q}_j}^{h,H}} \left\{ \delta_{ij} m_q^2 \left[B_0(m_{\tilde{q}_i}^2; M_{\tilde{g}}, m_q) + B_0(m_{\tilde{q}_j}^2; M_{\tilde{g}}, m_q) + 2B_0(M_{h,H}^2; m_q, m_q) \right. \right. \\ &\quad \left. \left. + (2M_{\tilde{g}}^2 + 2m_q^2 - m_{\tilde{q}_i}^2 - m_{\tilde{q}_j}^2) C_0(m_{\tilde{q}_i}^2, M_{h,H}^2, m_{\tilde{q}_j}^2; M_{\tilde{g}}, m_q, m_q) \right] \right. \\ &\quad \left. + \mathcal{R}_{ij} M_{\tilde{g}} m_q \left[(M_{h,H}^2 - 4m_q^2) C_0(m_{\tilde{q}_i}^2, M_{h,H}^2, m_{\tilde{q}_j}^2; M_{\tilde{g}}, m_q, m_q) \right. \right. \\ &\quad \left. \left. - B_0(m_{\tilde{q}_i}^2; M_{\tilde{g}}, m_q) - B_0(m_{\tilde{q}_j}^2; M_{\tilde{g}}, m_q) \right] \right\} \end{aligned}$$

$$\begin{aligned}
C_2^A &= \frac{g_q^A}{g_{\tilde{q}_i \tilde{q}_j}^A} \left\{ m_q^2 \sin 2\theta_q \left[B_0(m_{\tilde{q}_i}^2; M_{\tilde{g}}, m_q) - B_0(m_{\tilde{q}_j}^2; M_{\tilde{g}}, m_q) \right. \right. \\
&\quad \left. \left. + (m_{\tilde{q}_i}^2 - m_{\tilde{q}_j}^2) C_0(m_{\tilde{q}_i}^2, M_A^2, m_{\tilde{q}_j}^2; M_{\tilde{g}}, m_q, m_q) \right] \right. \\
&\quad \left. - (-1)^i M_{\tilde{g}} m_q \left[M_A^2 C_0(m_{\tilde{q}_i}^2, M_A^2, m_{\tilde{q}_j}^2; M_{\tilde{g}}, m_q, m_q) \right. \right. \\
&\quad \left. \left. - B_0(m_{\tilde{q}_i}^2; M_{\tilde{g}}, m_q) - B_0(m_{\tilde{q}_j}^2; M_{\tilde{g}}, m_q) \right] \right\} \\
C_3^{h,H} &= -\frac{\mathcal{S}_{ik} g_{\tilde{q}_k \tilde{q}_i}^{h,H} \mathcal{S}_{lj}}{g_{\tilde{q}_i \tilde{q}_j}^{h,H}} B_0(M_{h,H}^2; m_{\tilde{q}_k}, m_{\tilde{q}_i}) \\
C_3^A &= B_0(M_A^2; m_{\tilde{q}_i}, m_{\tilde{q}_j}) \\
\frac{\alpha_s}{\pi} C_{CT}^{h,H} &= \delta Z_{ii} + \delta Z_{jj} + \frac{2}{g_{\tilde{q}_i \tilde{q}_j}^{h,H}} \left[\frac{\partial g_{\tilde{q}_i \tilde{q}_j}^{h,H}}{\partial m_q} \delta m_q + \frac{\partial g_{\tilde{q}_i \tilde{q}_j}^{h,H}}{\partial A_q} \delta \bar{A}_q + \mathcal{T}_{ij} \Delta \theta_q \right] \\
\frac{\alpha_s}{\pi} C_{CT}^A &= \delta Z_{ii} + \delta Z_{jj} + \frac{2}{g_{\tilde{q}_i \tilde{q}_j}^A} \left[\frac{\partial g_{\tilde{q}_i \tilde{q}_j}^A}{\partial m_q} \delta m_q + \frac{\partial g_{\tilde{q}_i \tilde{q}_j}^A}{\partial A_q} \delta \bar{A}_q \right] \\
C_{real}^\Phi &= C_F \Gamma(1 + \epsilon) \left(\frac{4\pi \bar{\mu}^2}{M_\Phi^2} \right)^\epsilon \left\{ \frac{1 - \rho_i - \rho_j}{2\beta} \left[\frac{\log x_0}{\epsilon} + \log x_0 \log \frac{\rho_i \rho_j x_0}{\beta^4} \right. \right. \\
&\quad \left. \left. - \frac{1}{2} \log^2 x_1 - \frac{1}{2} \log^2 x_2 + 4Li_2 \left(\frac{1 - x_0}{-x_0} \right) - 2Li_2(1 - x_1) - 2Li_2(1 - x_2) \right] \right. \\
&\quad \left. + \frac{1}{\epsilon} + \log \frac{\rho_i \rho_j}{\beta^4} + 4 - \frac{1 + \rho_i + \rho_j}{2\beta} \log x_0 + \frac{\rho_i \log x_1 + \rho_j \log x_2}{\beta} \right\}, \quad (39)
\end{aligned}$$

where in C_{real} we used the abbreviations $\beta = \sqrt{\lambda_{ij}}$ with the two-body phase-space function λ_{ij} of Eq. (34) and

$$x_0 = \frac{1 - \rho_i - \rho_j - \beta}{1 - \rho_i - \rho_j + \beta}, \quad x_1 = \frac{1 - \rho_i + \rho_j - \beta}{1 - \rho_i + \rho_j + \beta}, \quad x_2 = \frac{1 + \rho_i - \rho_j - \beta}{1 + \rho_i - \rho_j + \beta} \quad (40)$$

with $\rho_i = m_{\tilde{q}_i}^2/M_\Phi^2$. The two mixing matrices \mathcal{R} and \mathcal{S} used in the coefficients $C_2^{h,H}$ and $C_3^{h,H}$ are given by

$$\mathcal{R} = \begin{pmatrix} \sin 2\theta_q & \cos 2\theta_q \\ \cos 2\theta_q & -\sin 2\theta_q \end{pmatrix}, \quad \mathcal{S} = \begin{pmatrix} \cos 2\theta_q & -\sin 2\theta_q \\ -\sin 2\theta_q & -\cos 2\theta_q \end{pmatrix}. \quad (41)$$

The three-point function C_0 is defined as [16]

$$C_0(p_1^2, p_2^2, p_{12}^2; m_1, m_2, m_3) = \int \frac{d^n k}{(2\pi)^n} \frac{-i(4\pi)^2 \bar{\mu}^{2\epsilon}}{[k^2 - m_1^2][(k + p_1)^2 - m_2^2][(k + p_{12})^2 - m_3^2]} \quad (42)$$

with $p_{12} = p_1 + p_2$. The finite remainders of the mixing angle renormalization at the external squark legs can be cast into the form of the matrix

$$\mathcal{T} = \begin{pmatrix} 2g_{\tilde{q}_1 \tilde{q}_2}^\Phi & g_{\tilde{q}_1 \tilde{q}_1}^\Phi + g_{\tilde{q}_2 \tilde{q}_2}^\Phi \\ g_{\tilde{q}_1 \tilde{q}_1}^\Phi + g_{\tilde{q}_2 \tilde{q}_2}^\Phi & 2g_{\tilde{q}_1 \tilde{q}_2}^\Phi \end{pmatrix} \quad (43)$$

multiplied by the finite shift

$$\Delta\theta_q = \frac{\Re\Sigma_{12}(m_{\tilde{q}_2}^2)}{m_{\tilde{q}_2}^2 - m_{\tilde{q}_1}^2} - \delta\theta_q = \frac{1}{2}\Re e \frac{\Sigma_{12}(m_{\tilde{q}_2}^2) - \Sigma_{12}(m_{\tilde{q}_1}^2)}{m_{\tilde{q}_2}^2 - m_{\tilde{q}_1}^2}, \quad (44)$$

which includes the corresponding anti-Hermitian counter term $\delta\theta_q$ of the mixing angle as given in Eq. (23). In Eq. (44) the singularity for $m_{\tilde{q}_2}^2 \rightarrow m_{\tilde{q}_1}^2$ is cancelled by the anti-Hermitian counter term. Finally the derivatives of the squark couplings $g_{\tilde{q}_i\tilde{q}_j}^\Phi$ to the Higgs bosons are given by

$$\begin{aligned} \frac{\partial g_{\tilde{q}_i\tilde{q}_j}^{h,H}}{\partial m_q} &= 2m_q g_q^{h,H} \delta_{ij} + \frac{g_{\tilde{q}_L\tilde{q}_R}^{h,H}}{m_q} \mathcal{R}_{ij} \\ \frac{\partial g_{\tilde{q}_i\tilde{q}_j}^{h,H}}{\partial A_q} &= \frac{m_q}{2} g_q^{h,H} \mathcal{R}_{ij} \\ \frac{\partial g_{\tilde{q}_1\tilde{q}_2}^A}{\partial m_q} &= -\frac{\partial g_{\tilde{q}_2\tilde{q}_1}^A}{\partial m_q} = \frac{g_{\tilde{q}_1\tilde{q}_2}^A}{m_q} \\ \frac{\partial g_{\tilde{q}_1\tilde{q}_2}^A}{\partial A_q} &= -\frac{\partial g_{\tilde{q}_2\tilde{q}_1}^A}{\partial A_q} = \frac{m_q}{2} g_q^A. \end{aligned} \quad (45)$$

The results for the coefficients C^Φ are ultraviolet and infrared finite after all individual contributions are added up since our renormalized mixing angles fulfill the relation $\sin^2 2\theta_q + \cos^2 2\theta_q = 1$ consistently. The scale of α_s in Eq.(39) is identified with the renormalization scale everywhere apart from the Δ_b term within the effective bottom mass of Eq. (8). It should be noted that our final results do not contain any leading $\text{tg}\beta$ -enhanced corrections of the Δ_b -type anymore due to our scheme choices of the effective masses and couplings at NLO. Due to this property the problems of a naive renormalization program have been solved consistently leading to moderate radiative corrections to the Higgs decay widths into squark-antisquark pairs as will be shown explicitly in the next section.

By using power counting arguments along the lines of Ref. [13] it can be shown that our approach resums all leading terms of $\mathcal{O}(\alpha_s^n \mu^n \text{tg}^n \beta)$ so that the residual HO corrections are free of these leading terms. In the current eigenstate basis there are three sources of terms proportional to $\text{tg}\beta$: (i) the Higgs couplings to squarks and quarks as in Table 1 and Eq. (26) which drop out in the relative corrections; (ii) off-diagonal mass insertions in the sbottom propagators which are power-suppressed by m_b/M_S due to the KLN theorem and the m_b/M_S structure of these insertions; (iii) potential $\text{tg}\beta$ -enhancements of the counter terms. The \overline{MS} renormalization of A_b as in Eq. (37) does not involve any $\text{tg}\beta$ enhanced corrections as can also be inferred from the beta functions of the RGEs for the trilinear couplings up to three-loop order [19]. The $\text{tg}\beta$ enhancement of the bottom-mass counter term entering the corresponding bottom Yukawa couplings involved in the Higgs couplings to bottom quarks and the sbottom mass matrix is explicitly absorbed in the effective bottom mass of Eq. (8) which contains the corresponding threshold correction Δ_b in resummed form [12, 13]. Therefore the counter terms δm_b and $\delta \bar{A}_b$ are free of $\text{tg}\beta$ enhanced corrections at all orders up to terms which are suppressed by m_b/M_S .

Close to the threshold $M_\Phi \sim m_{\tilde{q}_i} + m_{\tilde{q}_j}$ the NLO SUSY-QCD corrections develop Coulomb singularities,

$$C^\Phi \rightarrow \frac{C_F}{2} \frac{\pi^2}{\sqrt{\lambda_{ij}}} \frac{4m_{\tilde{q}_i}m_{\tilde{q}_j}}{(m_{\tilde{q}_i} + m_{\tilde{q}_j})^2} \quad \text{for } M_\Phi \rightarrow m_{\tilde{q}_i} + m_{\tilde{q}_j}, \quad (46)$$

which agrees with the usual Sommerfeld rescattering correction factor [21]. These singularities for $\sqrt{\lambda_{ij}} \rightarrow 0$ can be regularized by taking into account the finite decay widths of the squarks. Moreover, these Coulomb factors can be resummed systematically. Both effects are expected to be relevant close to threshold, but are beyond the scope of this paper.

On the other hand far above the threshold $M_\Phi \gg m_{\tilde{q}_{i,j}} \gg m_q$ the NLO corrections approach the asymptotic limit

$$\begin{aligned} C^\Phi &\rightarrow C_F \left\{ 2 \frac{m_q}{g_{\tilde{q}_i\tilde{q}_j}^\Phi} \frac{\partial g_{\tilde{q}_i\tilde{q}_j}^\Phi}{\partial m_q} \left[\frac{3}{4} \log \frac{\mu_R^2}{M_\Phi^2} - \frac{1}{4} \log \frac{M_\Phi^2}{M_S^2} + \frac{7}{4} + \gamma_q \right] \right. \\ &\quad \left. + 2 \frac{M_S}{g_{\tilde{q}_i\tilde{q}_j}^\Phi} \frac{\partial g_{\tilde{q}_i\tilde{q}_j}^\Phi}{\partial A_q} \left[-\log \frac{\mu_R^2}{M_S^2} + \frac{1}{4} \log^2 \frac{M_\Phi^2}{M_S^2} + \frac{\zeta_2}{2} - 2 \right] + \delta_\Phi \right\} \\ \delta_{h,H} &= \left[\frac{m_q}{g_{\tilde{q}_i\tilde{q}_j}^\Phi} \frac{\partial g_{\tilde{q}_i\tilde{q}_j}^\Phi}{\partial m_q} - 1 \right] \left[\log \frac{M_\Phi^2}{M_S^2} - 2 \right] + \frac{g_q^\Phi m_q^2}{g_{\tilde{q}_i\tilde{q}_j}^\Phi} \delta_{ij} \log \frac{M_\Phi^2}{M_S^2} \\ &\quad + \mathcal{T}_{ij} \frac{m_q \cos 2\theta_q}{M_S g_{\tilde{q}_i\tilde{q}_j}^\Phi} \left[1 - \frac{1}{2} \log \frac{M_S^2}{m_q^2} \right] \\ \delta_A &= 0, \end{aligned} \quad (47)$$

where we have identified all supersymmetric masses, $M_S = m_{\tilde{q}_1} = m_{\tilde{q}_2} = M_{\tilde{g}}$, and neglected the quark mass against the other masses. The term γ_q is given by

$$\gamma_t = \frac{A_t - \mu/\text{tg}\beta}{4M_S}, \quad \gamma_b = \frac{A_b}{4M_S} \quad (48)$$

thus confirming the absence of large corrections of $\mathcal{O}(\alpha_s \mu \text{tg}\beta)^9$. The asymptotic result far above the threshold develops a double logarithmic contribution in the second square bracket of Eq. (47) which originates from the second diagram of Fig. 3 in the Sudakov limit. It cannot be absorbed in an appropriate choice of the renormalization scale μ_R but will cancel against the corresponding double logarithm of gluino radiation in association with quark-squark pairs in the large Higgs mass limit which has not been taken into account in this work. In the following we will identify μ_R with the corresponding Higgs mass M_Φ as the central scale choice.

⁹In the on-shell scheme, which relates the renormalization of A_q to the on-shell quark and squark mass as well as the mixing angle counter terms as in Eq. (21) and renormalizes the quark mass on-shell, large corrections of $\mathcal{O}(\alpha_s \mu^2 \text{tg}^2 \beta)$ emerge for the partial Higgs decay widths into squarks.

4 Numerical Results

The numerical analysis of the neutral Higgs boson decays into stop and sbottom pairs is performed for two MSSM scenarios, one close to the one of Ref. [10] where we lifted the gluino and squark masses of the first two generations beyond the mass bounds from the LHC [22], and a second scenario with large SUSY-breaking masses and large mixing in the stop sector as representative cases:

$$\begin{aligned}
\text{A)} \quad & Q_0 = 300 \text{ GeV}, \\
& \text{tg}\beta = 30, \quad \overline{M}_{\tilde{t}_L}(Q_0) = \overline{M}_{\tilde{b}_L}(Q_0) = \overline{M}_{\tilde{\tau}_{L,R}}(Q_0) = 300 \text{ GeV}, \\
& \overline{M}_{\tilde{t}_R}(Q_0) = 270 \text{ GeV}, \quad \overline{M}_{\tilde{b}_R}(Q_0) = 330 \text{ GeV}, \\
& \overline{M}_{\tilde{q}_{L,R}}(Q_0) = \overline{M}_{\tilde{\ell}_{L,R}}(Q_0) = M_{\tilde{g}} = 1 \text{ TeV}, \quad \bar{A}_t(Q_0) = 150 \text{ GeV}, \\
& \bar{A}_b(Q_0) = -700 \text{ GeV}, \quad \bar{A}_\tau(Q_0) = 1 \text{ TeV}, \quad M_2 = 1 \text{ TeV}, \quad \mu = 260 \text{ GeV} \\
\\
\text{B)} \quad & Q_0 = 500 \text{ GeV}, \\
& \text{tg}\beta = 30, \quad \overline{M}_{\tilde{t}_{L,R}}(Q_0) = \overline{M}_{\tilde{b}_{L,R}}(Q_0) = \overline{M}_{\tilde{\tau}_{L,R}}(Q_0) = 500 \text{ GeV}, \\
& \overline{M}_{\tilde{q}_{L,R}}(Q_0) = \overline{M}_{\tilde{\ell}_{L,R}}(Q_0) = M_{\tilde{g}} = 1 \text{ TeV}, \quad \bar{A}_t(Q_0) = \bar{A}_b(Q_0) = -1.5 \text{ TeV}, \\
& \bar{A}_\tau(Q_0) = 0, \quad M_2 = 500 \text{ GeV}, \quad \mu = 500 \text{ GeV}, \tag{49}
\end{aligned}$$

where $\overline{M}_{\tilde{q}_{L,R}}(Q_0)$ and $\overline{M}_{\tilde{\ell}_{L,R}}(Q_0)$ denote the squark and slepton mass parameters of the first two generations. The results of this work have been implemented in the program HDECAY [23] which calculates the MSSM Higgs decay widths and branching ratios including the relevant higher-order corrections [20]. We use the RG-improved two-loop expressions for the Higgs masses and couplings of Ref. [24] which yield predictions for the Higgs boson masses that agree with the diagrammatic calculations of Ref. [2] within 3–4% in general. Thus the leading one- and two-loop corrections have been included in the Higgs masses and the effective mixing angle α . Consistency of our scheme with the scheme and scale choices of Ref. [24] requires the evolution of our sbottom parameters \bar{A}_b and $\overline{M}_{\tilde{b}_{L/R}}$ to the scale

$$Q_b = \max \left\{ \sqrt{\overline{M}_{\tilde{b}_L}^2(Q_0) + \overline{m}_b^2(m_t)}, \sqrt{\overline{M}_{\tilde{b}_R}^2(Q_0) + \overline{m}_b^2(m_t)} \right\} \tag{50}$$

and the stop parameters \bar{A}_t and $\overline{M}_{\tilde{t}_{L/R}}$ to the scale

$$Q_t = \max \left\{ \sqrt{\overline{M}_{\tilde{t}_L}^2(Q_0) + \overline{m}_t^2(m_t)}, \sqrt{\overline{M}_{\tilde{t}_R}^2(Q_0) + \overline{m}_t^2(m_t)} \right\}. \tag{51}$$

Since the scales Q_0 and $Q_{b/t}$ are of similar order of magnitude we neglect resummation effects so that the relations are given by¹⁰

$$\begin{aligned}
\bar{A}_b(Q_b) &= \bar{A}_b(Q_0) + \left\{ C_F \frac{\alpha_s(Q_0)}{\pi} M_3(Q_0) + \frac{3}{2} \frac{\alpha_t}{\pi} \bar{A}_t(Q_0) + \frac{\alpha_b}{4\pi} \bar{A}_b(Q_0) \right\} \log \frac{Q_b^2}{Q_0^2} \\
\overline{M}_{\bar{b}_L}^2(Q_b) &= \overline{M}_{\bar{b}_L}^2(Q_0) + \left\{ -C_F \frac{\alpha_s(Q_0)}{\pi} M_3^2(Q_0) + \frac{1}{4} \left[\frac{\alpha_t}{\pi} X_t + \frac{\alpha_b}{\pi} X_b \right] \right\} \log \frac{Q_b^2}{Q_0^2} \\
\overline{M}_{\bar{b}_R}^2(Q_b) &= \overline{M}_{\bar{b}_L}^2(Q_0) + \left\{ -C_F \frac{\alpha_s(Q_0)}{\pi} M_3^2(Q_0) + \frac{\alpha_b}{4\pi} X_b \right\} \log \frac{Q_b^2}{Q_0^2} \\
\bar{A}_t(Q_t) &= \bar{A}_t(Q_0) + \left\{ C_F \frac{\alpha_s(Q_0)}{\pi} M_3(Q_0) + \frac{\alpha_t}{4\pi} \bar{A}_t(Q_0) + \frac{3}{2} \frac{\alpha_b}{\pi} \bar{A}_b(Q_0) \right\} \log \frac{Q_t^2}{Q_0^2} \\
\overline{M}_{\bar{t}_L}^2(Q_t) &= \overline{M}_{\bar{t}_L}^2(Q_0) + \left\{ -C_F \frac{\alpha_s(Q_0)}{\pi} M_3^2(Q_0) + \frac{1}{4} \left[\frac{\alpha_t}{\pi} X_t + \frac{\alpha_b}{\pi} X_b \right] \right\} \log \frac{Q_t^2}{Q_0^2} \\
\overline{M}_{\bar{t}_R}^2(Q_t) &= \overline{M}_{\bar{t}_L}^2(Q_0) + \left\{ -C_F \frac{\alpha_s(Q_0)}{\pi} M_3^2(Q_0) + \frac{\alpha_t}{4\pi} X_t \right\} \log \frac{Q_t^2}{Q_0^2}
\end{aligned} \tag{52}$$

with the abbreviations

$$\begin{aligned}
\alpha_b &= \frac{\overline{m}_b^2(Q_0)}{2\pi v^2 \cos^2 \beta} \\
\alpha_t &= \frac{\overline{m}_t^2(Q_0)}{2\pi v^2 \sin^2 \beta} \\
X_b &= \overline{M}_{\bar{b}_L}^2(Q_0) + \overline{M}_{\bar{b}_R}^2(Q_0) + M_{H_1}^2 + \bar{A}_b^2(Q_0) \\
X_t &= \overline{M}_{\bar{t}_L}^2(Q_0) + \overline{M}_{\bar{t}_R}^2(Q_0) + M_{H_2}^2 + \bar{A}_t^2(Q_0)
\end{aligned} \tag{53}$$

and the soft SUSY-breaking Higgs mass parameters

$$\begin{aligned}
M_{H_1}^2 &= M_A^2 \sin^2 \beta - \frac{M_Z^2}{2} \cos 2\beta - \mu^2 \\
M_{H_2}^2 &= M_A^2 \cos^2 \beta + \frac{M_Z^2}{2} \cos 2\beta - \mu^2.
\end{aligned} \tag{54}$$

The top pole mass has been taken as $m_t = 172.6$ GeV, while the bottom quark pole mass has been chosen to be $m_b = 4.60$ GeV, which corresponds to a \overline{MS} mass $\overline{m}_b(\overline{m}_b) = 4.26$ GeV. The strong coupling constant has been normalized to $\alpha_s(M_Z) = 0.118$ which corresponds to the QCD scale $\Lambda_5 = 226.2$ MeV for 5 active flavours. The related SUSY–QCD scale Λ_{SUSY} of Eq. (29) amounts to $\Lambda_{SUSY} = 2.028$ keV in scenario A and $\Lambda_{SUSY} = 1.756$ keV in scenario B. The \overline{MS} masses involved in the scales $Q_{t,b}$ can be derived as $\overline{m}_t(m_t) = 165.1$ GeV and $\overline{m}_b(m_t) = 2.78$ GeV while the \overline{MS} gluino mass at the input

¹⁰Note that the left-handed soft supersymmetry-breaking squark mass parameters $\overline{M}_{\bar{b}_L}(Q_b)$ and $\overline{M}_{\bar{t}_L}(Q_t)$ are not equal, because they are evaluated for different scales Q_t and Q_b . We have modified the calculation of Ref. [24] to account for these differences consistently.

scale Q_0 amounts to $M_3(Q_0) = 1.028$ TeV in scenario A and $M_3(Q_0) = 1.006$ TeV in scenario B. The squark masses in the two scenarios amount in particular to

$$\begin{aligned}
\text{A)} \quad & m_{\tilde{t}_1} = 165.5 \text{ GeV}, \quad m_{\tilde{t}_2} = 278.0 \text{ GeV}, \quad m_{\tilde{b}_1} = 182.5 \text{ GeV}, \quad m_{\tilde{b}_2} = 265.6 \text{ GeV}, \\
& m_{\tilde{u}_L} = 989.8 \text{ GeV}, \quad m_{\tilde{u}_R} = 990.7 \text{ GeV}, \quad m_{\tilde{d}_L} = 993.1 \text{ GeV}, \quad m_{\tilde{d}_R} = 991.6 \text{ GeV} \\
\text{B)} \quad & m_{\tilde{t}_1} = 202.1 \text{ GeV}, \quad m_{\tilde{t}_2} = 708.0 \text{ GeV}, \quad m_{\tilde{b}_1} = 473.0 \text{ GeV}, \quad m_{\tilde{b}_2} = 536.3 \text{ GeV}, \\
& m_{\tilde{u}_L} = 1.011 \text{ TeV}, \quad m_{\tilde{u}_R} = 1.012 \text{ TeV}, \quad m_{\tilde{d}_L} = 1.014 \text{ TeV}, \quad m_{\tilde{d}_R} = 1.012 \text{ TeV}, \quad (55)
\end{aligned}$$

where $m_{\tilde{u}_{L/R}}$ and $m_{\tilde{d}_{L/R}}$ denote the up- and down-type squark masses of the first two generations.

In Fig. 5 we display the results for the partial decay widths of the heavy neutral Higgs particles into stop pairs and the relative corrections in scenario A. Since the stops are moderately heavy all decay modes are kinematically allowed for Higgs masses above about 560 GeV. The partial decay widths range at the few GeV level and turn out to be similar for all Higgs bosons above the corresponding thresholds except the scalar Higgs decay widths into non-diagonal stop pairs which are smaller. Apart from the Coulomb singularities at threshold the SUSY–QCD corrections are of moderate size in our scheme. Similar results have been obtained for the neutral Higgs boson decay widths into sbottom pairs as shown in Fig. 6. The moderate size of the full SUSY–QCD corrections confirms the proper absorption of the Δ_b terms as in Eq. (8). If the trilinear coupling A_b and the bottom quark mass m_b would be renormalized in the on-shell scheme the SUSY–QCD corrections would increase the LO results by more than an order of magnitude so that the result in the on-shell scheme becomes totally unreliable [10, 25]. The partial widths of the non-diagonal Higgs decays $H \rightarrow \tilde{b}_1 \bar{\tilde{b}}_2, \tilde{b}_2 \bar{\tilde{b}}_1$ are small, since the mixing factor $\cos 2\theta_b$ is small and thus the contributions of the left-right couplings $g_{b_L \tilde{b}_R}^H$ are suppressed, while the diagonal couplings $g_{b_L \tilde{b}_L}^H$ and $g_{b_R \tilde{b}_R}^H$ cancel each other to a large extent in the evaluation of the coupling $g_{b_1 \tilde{b}_2}^H$ of Eq. (7). Using the scheme of Ref. [17] for the mixing angle, i.e. defining the mixing angle counter terms as $\delta\theta_q = \Re e \Sigma_{12}(Q^2)/(m_{\tilde{q}_2}^2 - m_{\tilde{q}_1}^2)$ with $Q^2 = m_{\tilde{q}_1}^2$ or $Q^2 = m_{\tilde{q}_2}^2$, the results agree with ours within less than 1%¹¹.

In order to obtain an estimate of the residual theoretical uncertainties we show the renormalization scale dependence of the partial decay widths into stop and sbottom pairs in Fig. 7. The scale dependences of the partial decay widths into stop and sbottom pairs are significantly reduced at NLO. Varying the renormalization scale by a factor of 2 around the central scale $\mu_R = M_{H/A}$ the theoretical uncertainties can be estimated as 5–10% for decays into stop and sbottom pairs at NLO.

Fig. 8 displays the corresponding branching ratios of the dominant decay modes of the heavy scalar and the pseudoscalar Higgs boson in scenario A. It is clearly visible that the decays into stop and sbottom pairs belong to the dominant decay modes for masses above about 300–400 GeV, i.e. where they are kinematically allowed, reaching branching

¹¹The results using the tree-level like mixing angle $\tilde{\theta}_q$ of Eq. (13) develop sizeable differences to the results in our scheme for squark masses $m_{\tilde{q}_{1,2}}$ close to each other, where the partial decay widths $H \rightarrow \tilde{q}_1 \bar{\tilde{q}}_2, \tilde{q}_2 \bar{\tilde{q}}_1$ turn out to be negative thus signaling a basic problem with the tree-level-like mixing angle.

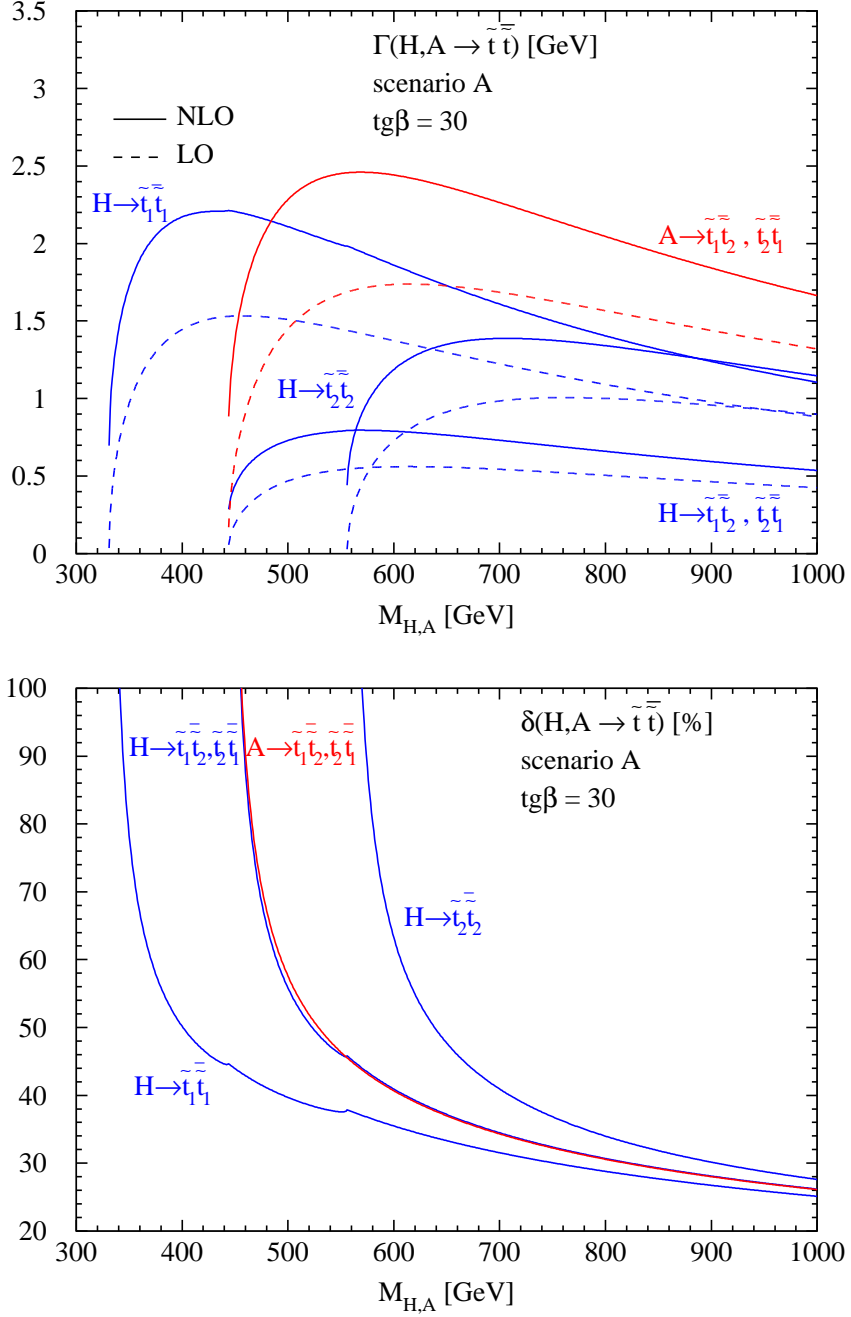


Figure 5: *SUSY-QCD corrected partial decay widths (upper) and the relative SUSY-QCD corrections (lower) of the heavy scalar and the pseudoscalar MSSM Higgs boson decays to stop pairs as functions of the corresponding Higgs masses for $\tan\beta = 30$ in scenario A. The full curves include the SUSY-QCD corrections, while the dashed ones are the LO results. The small kinks originate from the thresholds of the other stops in the virtual corrections.*

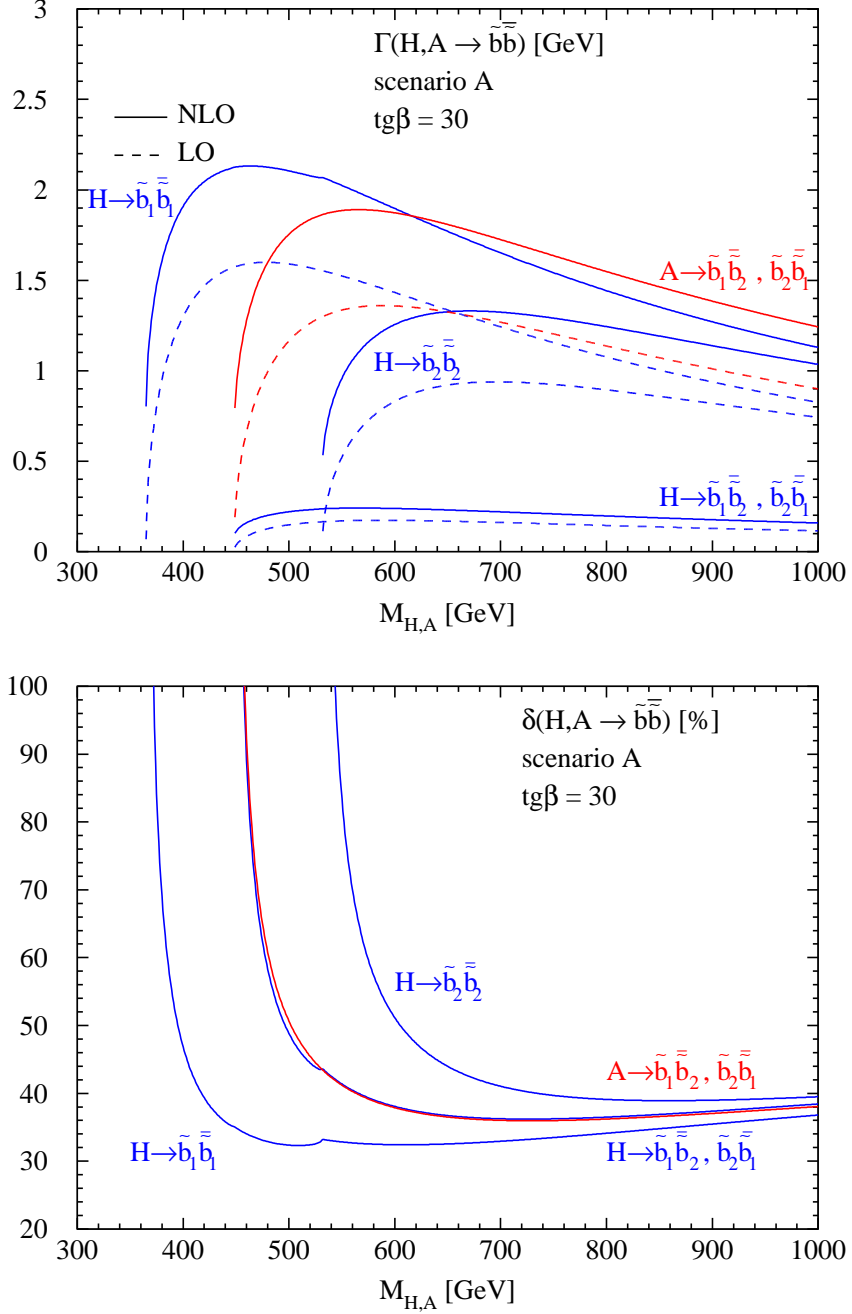


Figure 6: *SUSY-QCD* corrected partial decay widths (upper) and the relative *SUSY-QCD* corrections (lower) of the heavy scalar and the pseudoscalar MSSM Higgs boson decays to sbottom pairs as functions of the corresponding Higgs masses for $\tan\beta = 30$ in scenario A. The full curves include the *SUSY-QCD* corrections, while the dashed ones are the LO results. The small kinks originate from the thresholds of the other sbottoms in the virtual corrections.

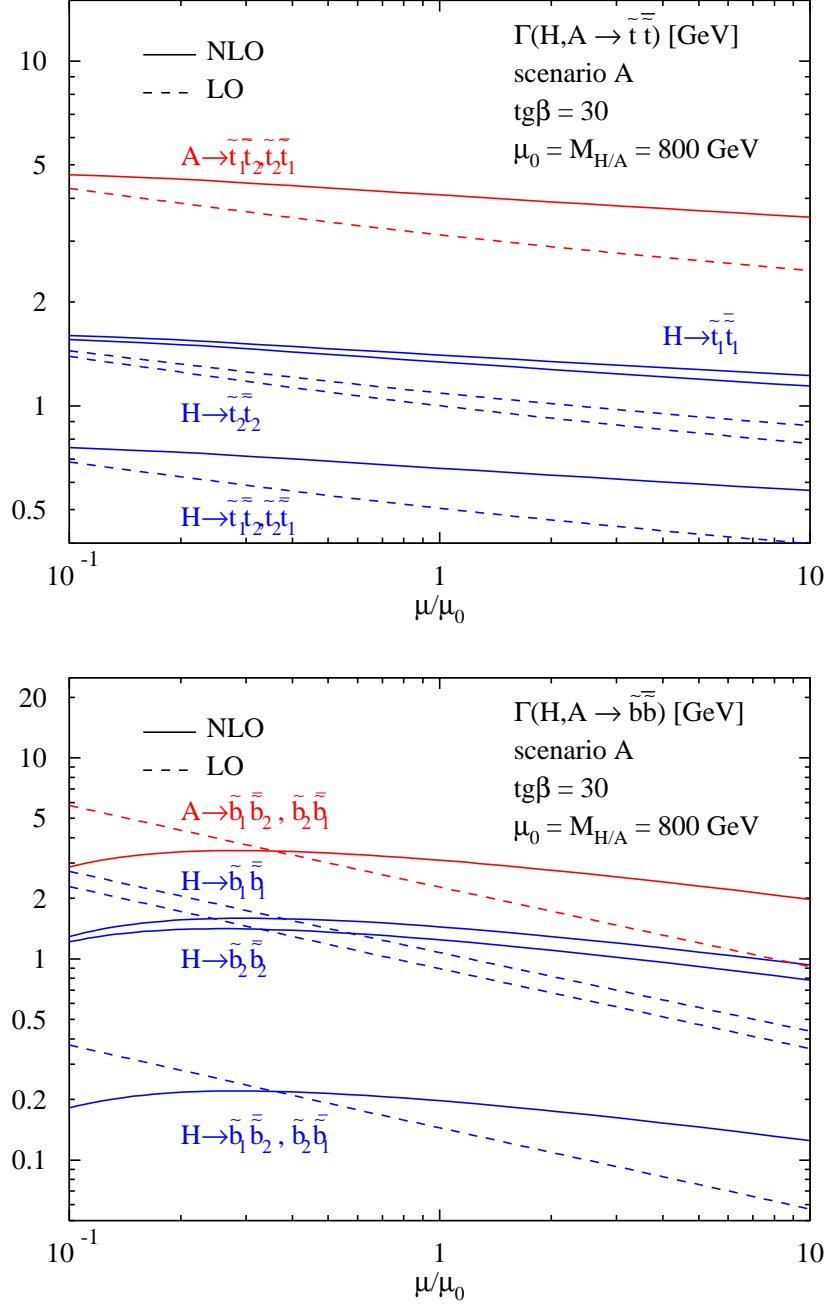


Figure 7: Scale dependences of the partial decay widths into stop pairs (upper) and sbottom pairs (lower) as functions of the renormalization scale in units of the central scale $\mu_0 = M_{H/A}$ in scenario A. The broken lines show the leading-order scale dependences and the full curves the NLO results.

ratios of up to about 50% in total. Moreover, in scenario A the decay modes into $\tilde{\tau}$'s and neutralinos play a significant role, too.

In Fig. 9 we display the final results for the scenario B. Since the masses $m_{\tilde{t}_2}, m_{\tilde{b}_{1,2}}$ are close to or larger than 500 GeV, the decay modes $H \rightarrow \tilde{t}_2\bar{\tilde{t}}_2, \tilde{b}_1\bar{\tilde{b}}_2, \tilde{b}_2\bar{\tilde{b}}_1, \tilde{b}_2\bar{\tilde{b}}_2$ are kinematically forbidden for $M_H \leq 1$ TeV. The partial decay widths of decays into stop and sbottom pairs range at the few GeV level as in scenario A once they are kinematically allowed. It can clearly be inferred from Fig. 9 that the SUSY–QCD corrections are of moderate size apart from the threshold regions where the Coulomb singularities enhance the size of the corrections. It should be noted that the results with the sbottom mixing angle renormalized via the tree-level relation of Eq. (21) would lead to unphysical negative partial decay widths for heavy scalar Higgs decays $H \rightarrow \tilde{b}_1\bar{\tilde{b}}_2, \tilde{b}_2\bar{\tilde{b}}_1$ for Higgs masses larger than 1 TeV, where these decay channels open up, so that this scheme is strongly disfavoured. These negative contributions can be traced back to the uncanceled artificial singularity for $m_{\tilde{b}_1} \sim m_{\tilde{b}_2}$ in the finite remainders $\Delta\theta_b$ of Eq. (44), if $\delta\theta_b$ is replaced by the counter term $\delta\tilde{\theta}_b$ of Eq. (21) [10].

In Fig. 10 we show the branching ratios of the heavy scalar and the pseudoscalar Higgs boson in scenario B as functions of the corresponding Higgs masses. As in scenario A the decay modes into stop and sbottom pairs play a significant role, once they are kinematically allowed. This starts to be the case for the heavy scalar Higgs boson H already for masses above about 400 GeV, where the decay into light stop mass eigenstates opens up. The pseudoscalar Higgs boson can only decay into mixed pairs of a light and heavy stop and sbottom eigenstates so that these decay modes open up for masses above 900 GeV. The decays into charginos and neutralinos contribute significantly for larger Higgs masses.

For smaller values of $\text{tg}\beta$ the decay modes $H \rightarrow hh, t\bar{t}$ and $A \rightarrow Zh, t\bar{t}$ play a significant role, while the decays into sbottom pairs are usually suppressed. However, the neutral Higgs boson decays into stop pairs still play a significant role and can even be the dominant heavy Higgs boson decays in a large Higgs mass range. The SUSY–QCD corrections to these decay modes are of similar size as in the scenarios with large values of $\text{tg}\beta$ analyzed in this work.

5 Conclusions

In this work we have analyzed the NLO SUSY–QCD corrections to heavy MSSM Higgs decays into stop and sbottom pairs and elaborated a consistent scheme and setup for the theoretical NLO results and the corresponding input parameters, i.e. the squark masses and their couplings to the Higgs bosons. A reliable determination of these corrections requires a proper treatment of contributions which are enhanced by $\text{tg}\beta$. The derivation of the input squark masses and couplings with NLO accuracy requires a modification of the tree-level relations among the stop and sbottom masses by higher-order corrections, if they should correspond to the physical pole masses. Since the size of these modifications depends on the MSSM parameters and pole masses themselves an iterative procedure

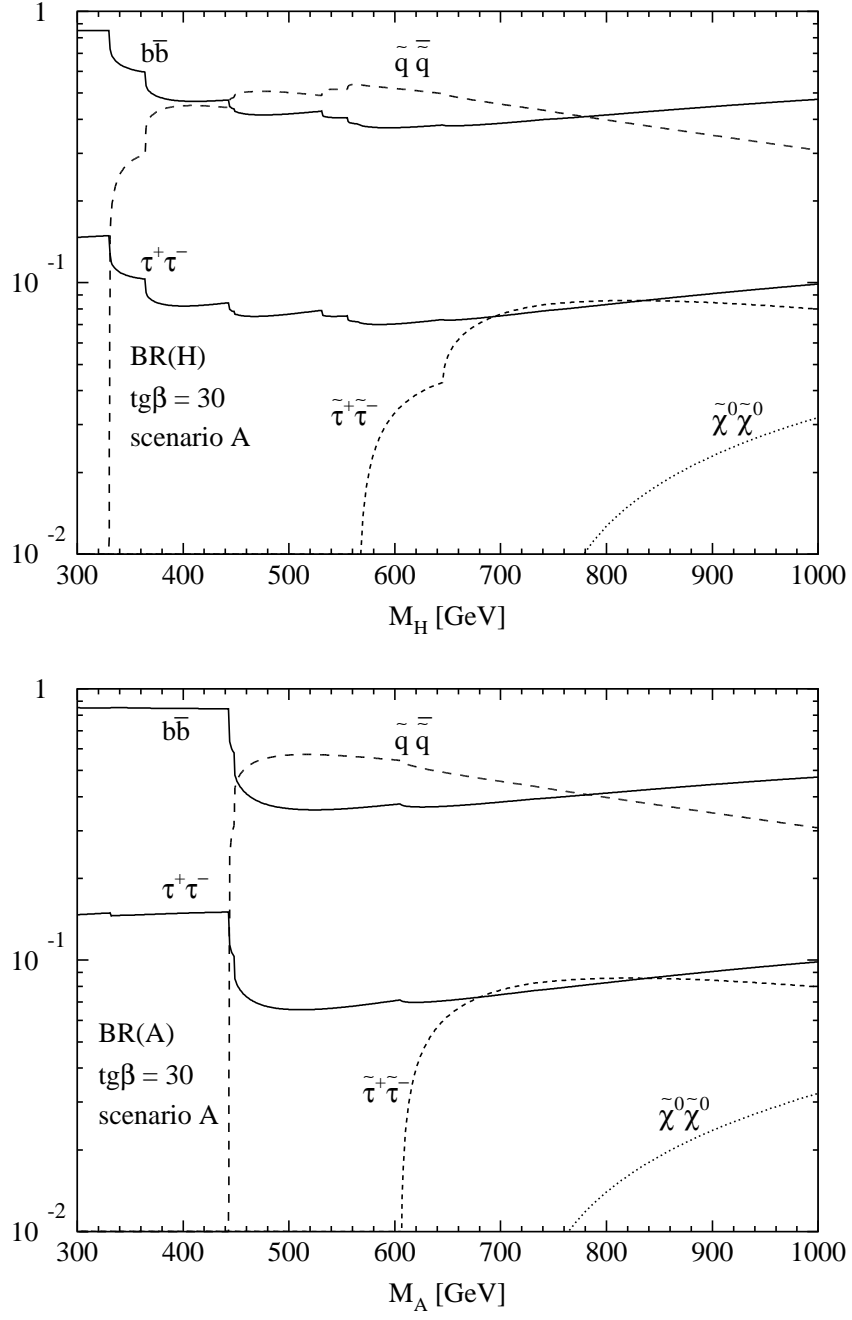


Figure 8: Branching ratios of the heavy scalar H and the pseudoscalar A MSSM Higgs bosons in scenario A as functions of the corresponding Higgs masses. The curves for decays into neutralinos $\tilde{\chi}^0\tilde{\chi}^0$ and squarks $\tilde{q}\tilde{q}$ represent the corresponding sums over all possible mass eigenstates.

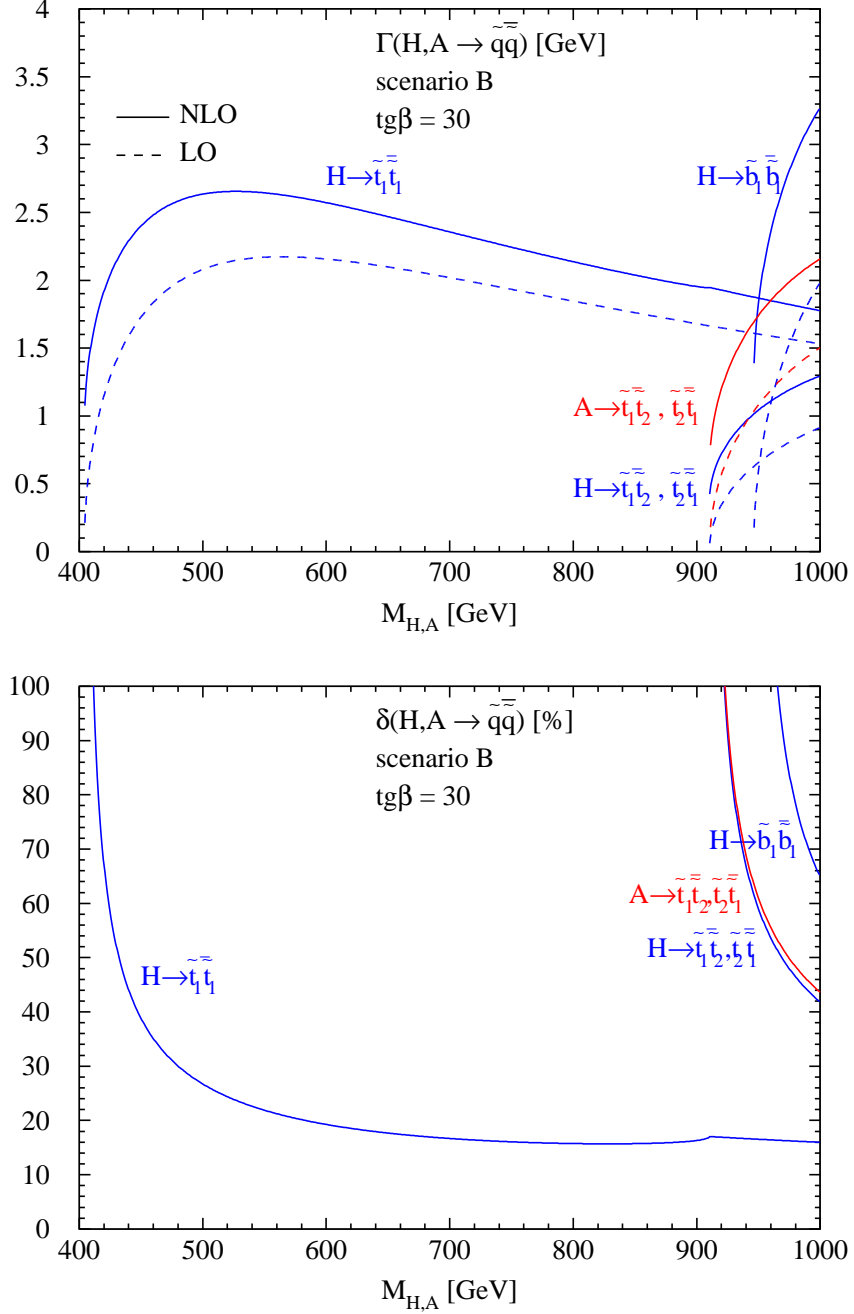


Figure 9: *SUSY-QCD* corrected partial decay widths (upper) and the relative *SUSY-QCD* corrections (lower) of the heavy scalar and the pseudoscalar MSSM Higgs boson decays to stop and sbottom pairs as functions of the corresponding Higgs masses for $\tan\beta = 30$ in scenario B. The full curves include the *SUSY-QCD* corrections, while the dashed ones are the LO results. The small kinks originate from the thresholds of the other stops in the virtual corrections.

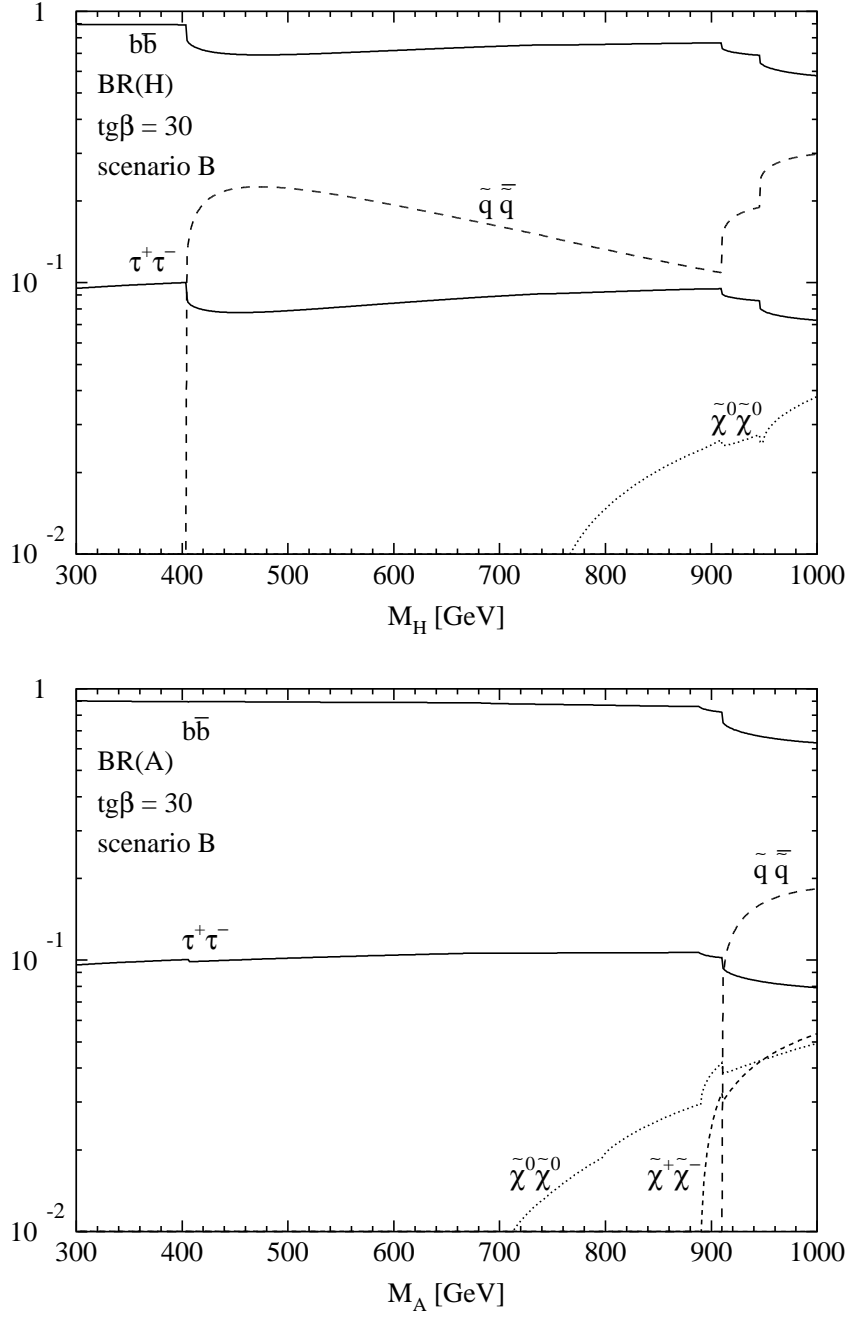


Figure 10: Branching ratios of the heavy scalar H and the pseudoscalar A MSSM Higgs bosons in scenario B as functions of the corresponding Higgs masses. The curves for decays into charginos $\tilde{\chi}^+\tilde{\chi}^-$, neutralinos $\tilde{\chi}^0\tilde{\chi}^0$ and squarks $\tilde{q}\tilde{q}$ represent the corresponding sums over all possible mass eigenstates.

should be applied. These iterations, however, do not converge for all scenarios so that we restricted the evaluation to a single iteration step. The final setup of the input parameters matches NLO accuracy consistently. A preferred choice of the scheme for the stop and sbottom mixing angles is the on-shell definition via the anti-Hermitian counter term which removes spurious singularities for nearly mass degenerate cases which drive the off-diagonal decays $H \rightarrow \tilde{b}_1 \tilde{b}_2$ to negative and thus unphysical values. The final NLO corrections are of moderate size apart from the expected Coulomb singularities at the decay thresholds. The residual theoretical uncertainties at NLO have been estimated to be 5–10%.

Note added in proof. During completion of this work Ref. [26] appeared which discusses several options for the renormalization of the stop and sbottom sector with NLO accuracy. Their treatment of the stop and sbottom sectors is different from our approach in particular for the effective bottom mass and the squark mixing angles.

Acknowledgments.

We are grateful to A. Djouadi, M. Mühlleitner, H. Rzehak and P.M. Zerwas for carefully reading our manuscript and useful comments.

References

- [1] P. Fayet, Nucl. Phys. **B90** (1975) 104, Phys. Lett. **B64** (1976) 159 and Phys. Lett. **B69** (1977) 489. S. Dimopoulos and H. Georgi, Nucl. Phys. **B193** (1981) 150; N. Sakai, Z. Phys. **C11** (1981) 153; K. Inoue, A. Kakuto, H. Komatsu and S. Takeshita, Prog. Theor. Phys. **67** (1982) 1889, Prog. Theor. Phys. **68** (1982) 927 [Erratum-ibid. **70** (1983) 330] and Prog. Theor. Phys. **71** (1984) 413.
- [2] See e.g. G. Degrassi, S. Heinemeyer, W. Hollik, P. Slavich and G. Weiglein, Eur. Phys. J. **C28** (2003) 133.
- [3] S. P. Martin, Phys. Rev. **D75** (2007) 055005; R. V. Harlander, P. Kant, L. Mihaila and M. Steinhauser, Phys. Rev. Lett. **100** (2008) 191602, Erratum *ibid.* **101** (2008) 039901; P. Kant, R. V. Harlander, L. Mihaila and M. Steinhauser, arXiv:1005.5709 [hep-ph].
- [4] S. Schael *et al.* [ALEPH, DELPHI, L3 and OPAL Collaborations], Eur. Phys. J. **C47** (2006) 547.
- [5] M. S. Carena *et al.* [Higgs Working Group Collaboration], arXiv:hep-ph/0010338.
- [6] ATLAS Collaboration, Technical Design Report, CERN–LHCC 99–14 (May 1999); G. L. Bayatian *et al.* [CMS Collaboration], J. Phys. **G34** (2007) 995.
- [7] A. Djouadi, J. Kalinowski, P. Ohmann and P. M. Zerwas, Z. Phys. **C74** (1997) 93.

- [8] A. Bartl, H. Eberl, K. Hidaka, T. Kon, W. Majerotto and Y. Yamada, Phys. Lett. **B402** (1997) 303; A. Arhrib, A. Djouadi, W. Hollik and C. Jünger, Phys. Rev. **D57** (1998) 5860.
- [9] C. Weber, K. Kovarik, H. Eberl and W. Majerotto, Nucl. Phys. **B776** (2007) 138.
- [10] H. Eberl, K. Hidaka, S. Kraml, W. Majerotto and Y. Yamada, Phys. Rev. **D62** (2000) 055006.
- [11] S.P. Martin and M.T. Vaughn, Phys. Lett. **B318** (1993) 331.
- [12] L. J. Hall, R. Rattazzi and U. Sarid, Phys. Rev. **D50** (1994) 7048; R. Hempfling, Phys. Rev. **D49** (1994) 6168; M. Carena, M. Olechowski, S. Pokorski and C. E. Wagner, Nucl. Phys. **B426** (1994) 269; M. Carena, D. Garcia, U. Nierste and C. E. Wagner, Nucl. Phys. **B577** (2000) 88.
- [13] J. Guasch, P. Häfliger and M. Spira, Phys. Rev. **D68** (2003) 115001.
- [14] D. Noth and M. Spira, Phys. Rev. Lett. **101** (2008) 181801 and arXiv:1001.1935 [hep-ph]; L. Mihaila and C. Reisser, JHEP **1008** (2010) 021.
- [15] A. Crivellin, L. Hofer, J. Rosiek, JHEP **1107** (2011) 017.
- [16] G. 't Hooft and M.J.G. Veltman, Nucl. Phys. **B153** (1979) 365; G. Passarino and M.J.G. Veltman, Nucl. Phys. **B160** (1979) 151.
- [17] W. Beenakker, R. Höpker, T. Plehn and P.M. Zerwas, Z. Phys. **C75** (1997) 349-356.
- [18] N. Baro, F. Boudjema, Phys. Rev. **D80** (2009) 076010.
- [19] S. P. Martin, M. T. Vaughn, Phys. Rev. **D50** (1994) 2282; Y. Yamada, Phys. Rev. **D50** (1994) 3537; I. Jack and D. R. T. Jones, Phys. Lett. **B333** (1994) 372; I. Jack, D. R. T. Jones, A. F. Kord, Phys. Lett. **B579** (2004) 180.
- [20] M. Spira, Fortsch. Phys. **46** (1998) 203; A. Djouadi, Phys. Rept. **459** (2008) 1.
- [21] A. Sommerfeld, *Atombau und Spektrallinien*, Vieweg, Braunschweig 1939.
- [22] V. Khachatryan *et al.* [CMS Collaboration], arXiv:1101.1628 [hep-ex]; The ATLAS Collaboration, arXiv:1102.2357 [hep-ex].
- [23] A. Djouadi, J. Kalinowski and M. Spira, Comput. Phys. Commun. **108** (1998) 56; A. Djouadi, J. Kalinowski, M. Mühlleitner and M. Spira, in J. M. Butterworth *et al.*, arXiv:1003.1643 [hep-ph]; A. Djouadi, M. M. Mühlleitner and M. Spira, Acta Phys. Polon. **B38** (2007) 635-644.
- [24] M.S. Carena, M. Quiros and C.E.M. Wagner, Nucl. Phys. **B461** (1996) 407.
- [25] Manuel Walser, Diploma Thesis, Zürich, 2003.
- [26] S. Heinemeyer, H. Rzehak and C. Schappacher, Phys. Rev. **D82** (2010) 075010.